CANM ACMN
The Canadian Association of Nuclear Medicine
Association canadienne de médecine nucléaire

Brain PET in 2019:
The Established, the Almost-There and the Future

Jean-Paul Soucy, MD, MSc
Director, PET Unit,
Montreal Neurological Institute.
Adjunct Professor, Neurology and Neurosurgery,
McGill University.
Associate Director, Bio-Imaging,
PERFORM Centre,
Concordia University
Professeur titulaire de clinique,
Radiologie, médecine nucléaire et radio-oncologie
Université de Montréal

JPS has served as consultant to:
GE Health Care
Biospective
Optina Diagnostics (no money received; conjoint grants)

None of the above affects this presentation

Plan/Objectives

- The established:
  ^{18}F-FDG: old, but still going strong!/ A quick, brief, not long, short discussion to remember that it's still the best we have

- The almost there:
  - Amyloid PET Imaging: good, work-in-progress/ Understand what it means to find plaques in the brain in order to define clinical indications
  - Tau imaging/ Recognize that it's great for research, and might also be for patients

- The future / Review some avenues that will keep us relevant

Positron Emission Tomography in the Study of Aging and Senile Dementia[1,2]

FERRIS, S. H., M. J. DE LEON, A. P. WOLF, T. FARKAS, D. R. CHRISTMAN, B. REISBERG, J. S. FOWLER, R. MACGREGOR, A. GOLDMAN, A. E. GEORGE AND S. RAMPAL. *Positron emission tomography in the study of aging and senile dementia.* NEUROBIOL. AGING 1(2) 127–131, [redacted].—^{18}F-2-deoxy-2-fluoro-D-glucose (^{18}FDG) is a positron emitting tracer for rate of glucose utilization in brain. When used in conjunction with positron emission tomography (PET), the PET-FDG technique permits *in vivo* quantitation of regional brain metabolism in man. We have applied this technique to the study of regional brain function in normal aging and senile dementia. Preliminary results for 7 patients with senile dementia of the Alzheimer's type (SDAT) and 3 elderly normal subjects indicated a large, statistically significant ($p<0.01$) diminution in rate of glucose utilization in SDAT. Furthermore, the degree of diminution in metabolic activity in SDAT was highly correlated with objective measures of degree of cognitive impairment. These results demonstrate the feasibility and potential utility of the PET-FDG technique for studying regional brain function in normal aging and dementia.

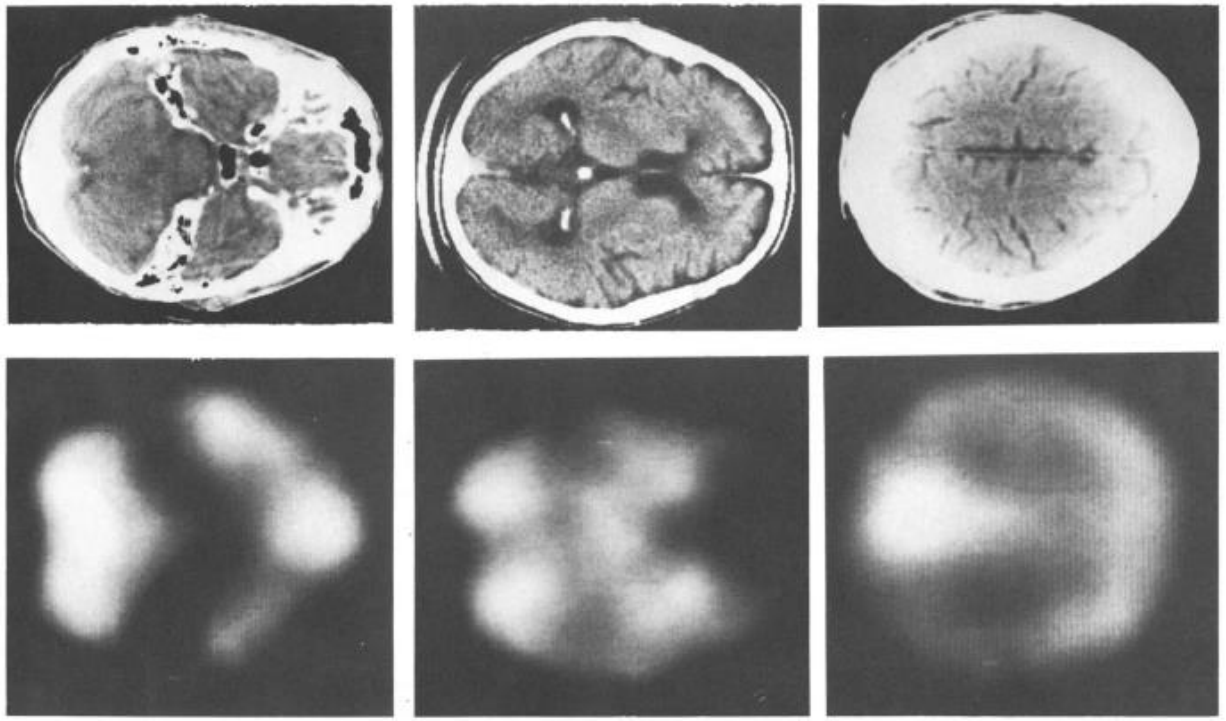

^{18}FDG and NCD: going back a long way …

^{18}F-FDG PET imaging shows

All neurodegenerative diseases affect synaptic transmission early in their evolution

And at least initially, this happens with a regionally recognizable pattern

- The presence or absence of synaptic dysfunction
- If present, its distribution can confirm the presence/absence of a neurodegenerative process and its nature
- However, the severity of a neurodegenerative condition CANNOT be assessed with this technique (cognitive reserve)

Polymodal associative cortices are typically the first to be affected

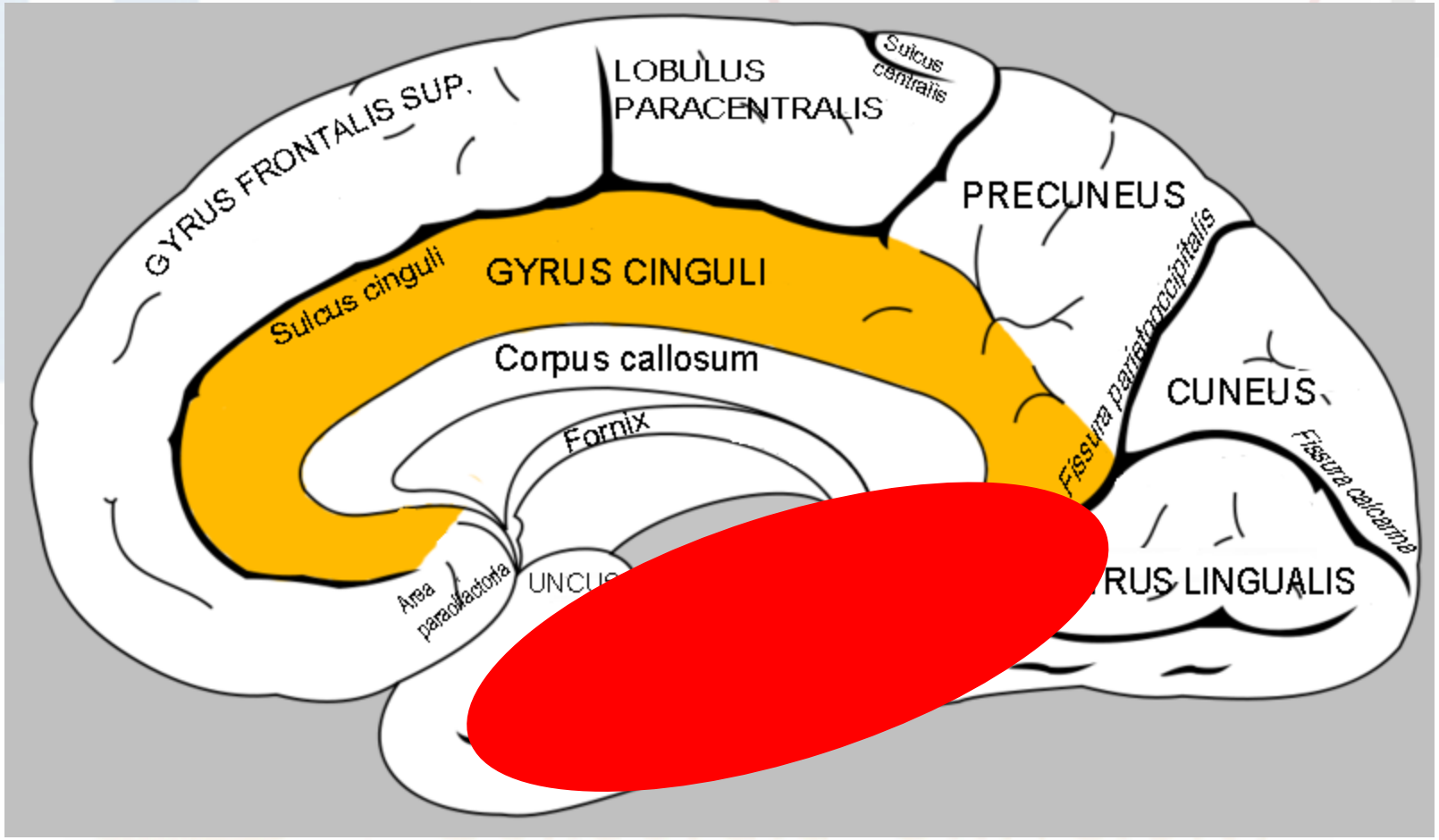

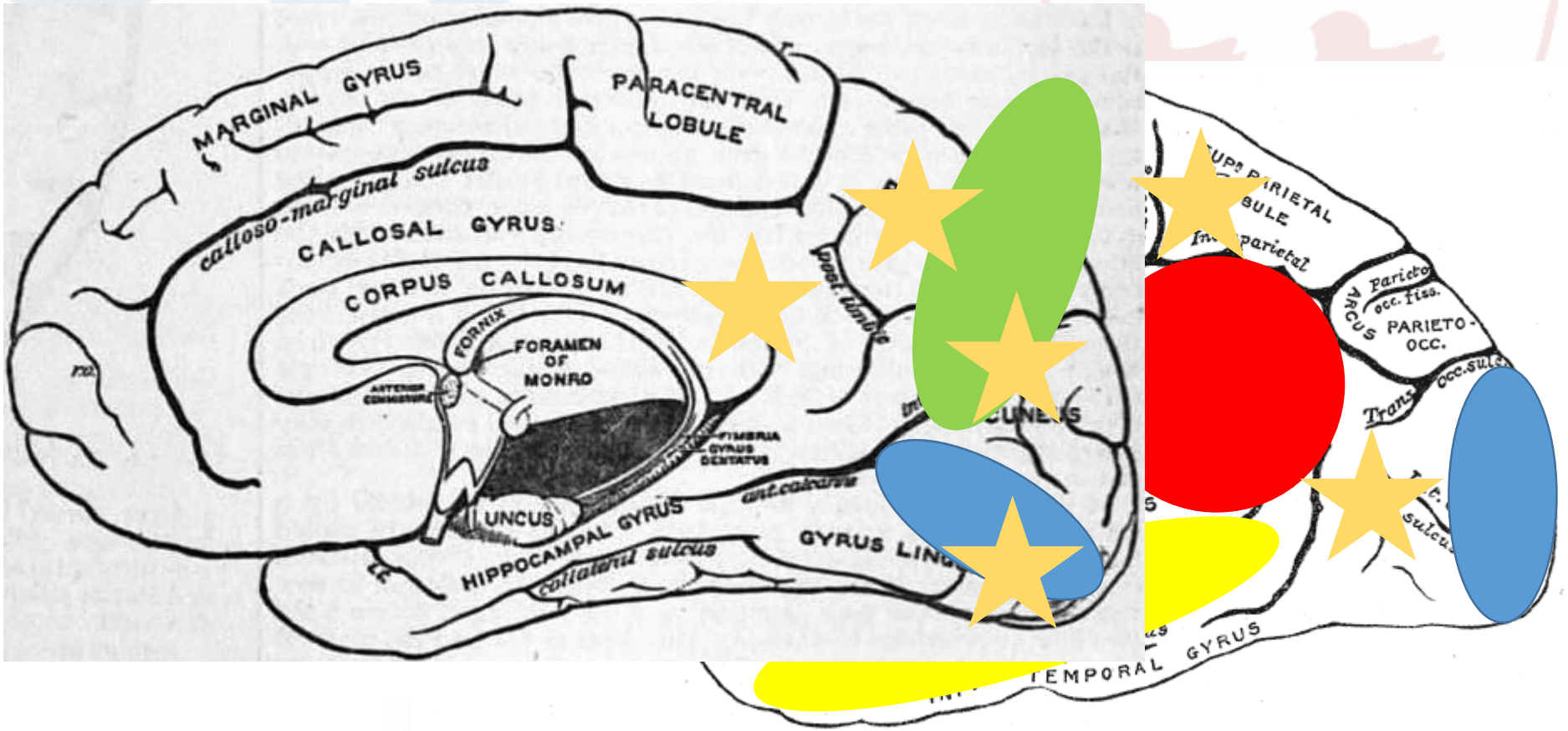

EXCEPTIONS!!

- LBDs and visual cortex
- ALS and M1
- CJD (+ bilateral)
- Some CBD cases (+ unilateral)

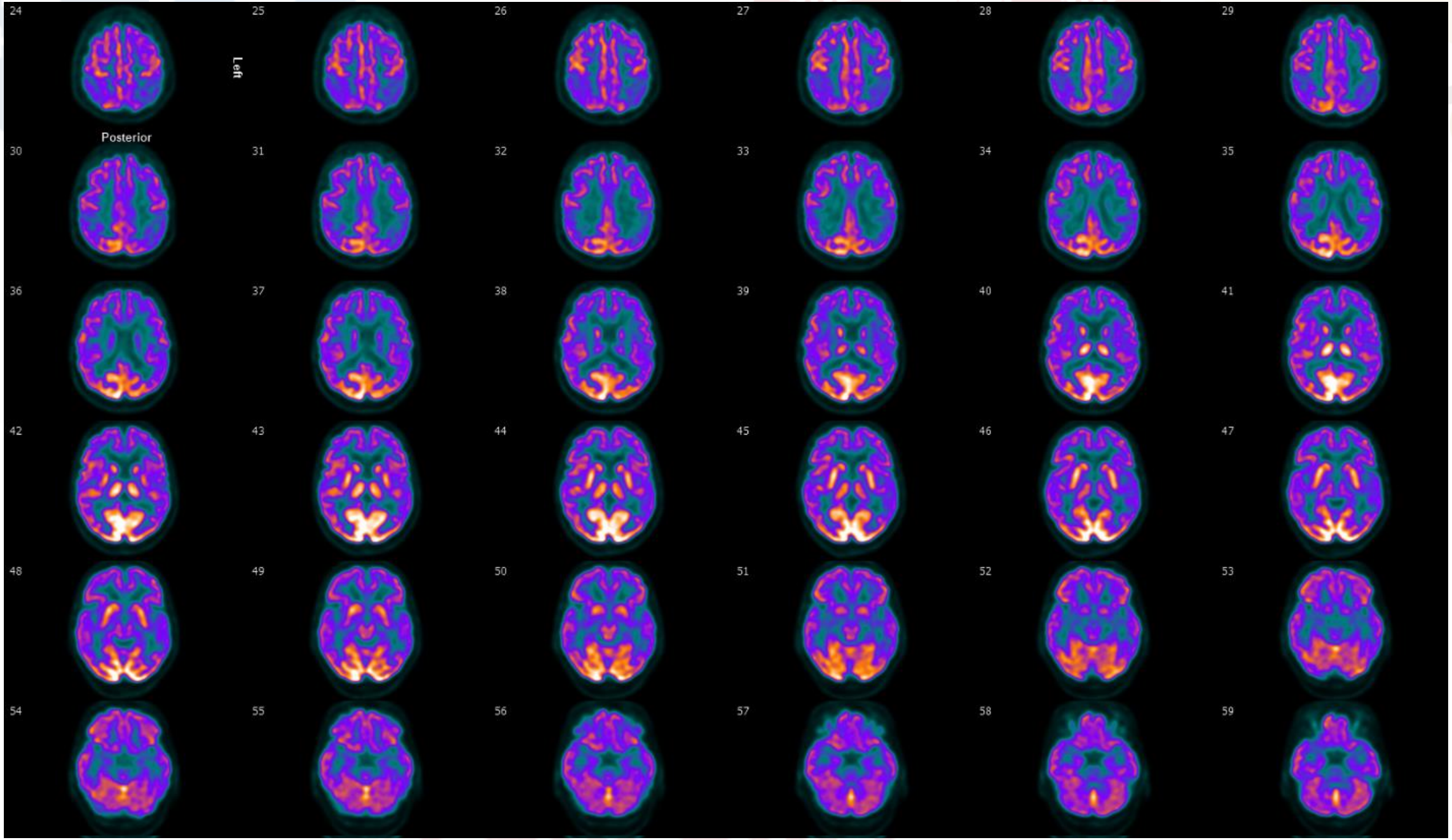
24
25
26
27
28
29
Left
Posterior
30
31
32
33
34
35
36
37
38
39
40
41
42
43
44
45
46
47
48
49
50
51
52
53
54
55
56
57
58
59

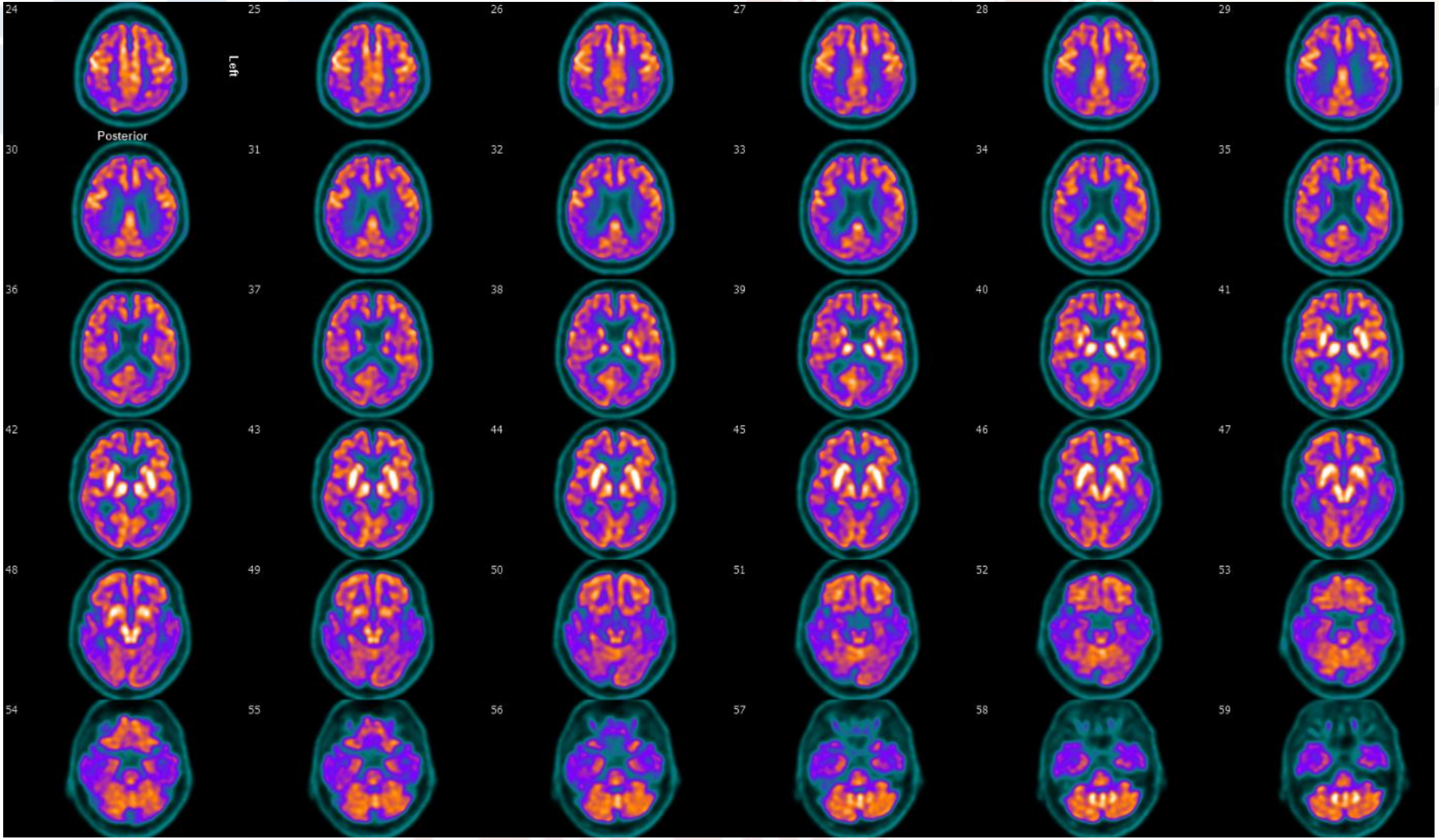
24
25
26
27
28
29
Left
Posterior
30
31
32
33
34
35
36
37
38
39
40
41
42
43
44
45
46
47
48
49
50
51
52
53
54
55
56
57
58
59

And this holds for

AD variants,

PSP,

MSA,

CBD,

PPA variants (semantic, non-fluent/agrammatical logopenic, etc…)

Confirmed on 100s of thousands subjects

You already know all of this!!

Here, we'll just review the

strenght of the evidence of FDG's usefulness

NEVER make a Dx based only on this (or equivalent)!!!!!

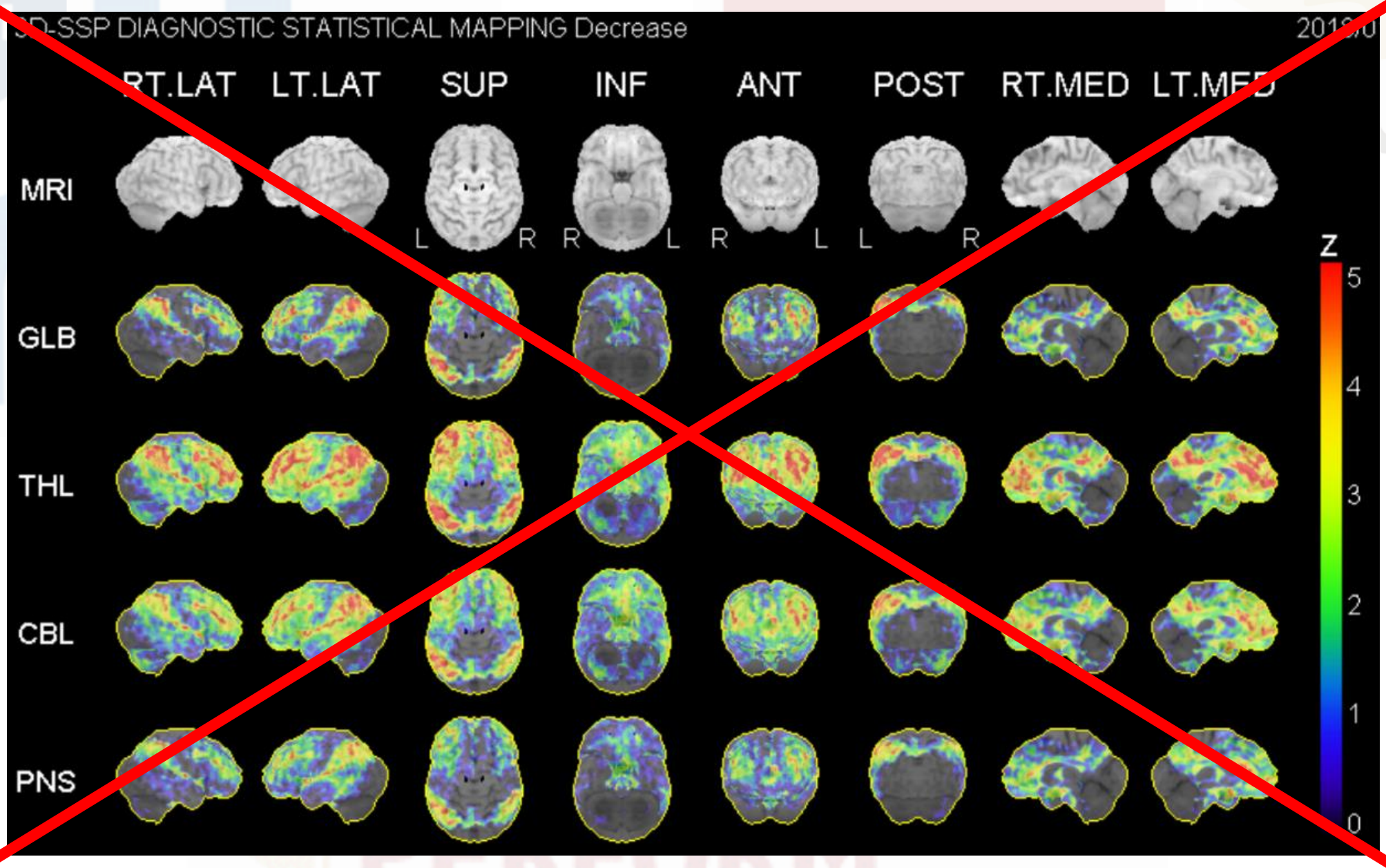

Just a pet peeve of mine before moving on …

Effectiveness and Safety of ^{18}F-FDG PET in the Evaluation of Dementia: A Review of the Recent Literature

Nicolaas I. Bohnen[1–3], David S.W. Djang[4], Karl Herholz[5], Yoshimi Anzai[6,7], and Satoshi Minoshima[6]

So, does FDG PET work clinically?
Here's a good review to start answering this question:

Imaging that can detect pathophysiologic change in the brain holds great promise for diagnostic assessment of patients with Alzheimer disease (AD) and dementia. Although a previous metaanalysis centering on literature from 1990 to 2000 showed a summary accuracy of 86% for ^{18}F-FDG PET for AD diagnosis, the cl f meth- odolo e since 2000 in as- sessm es that includ recruit- ment cohort studie ort the role o o other diagnostic information in the assessment of patients with symptoms of dementia. Findings are in line with recently revised diagnostic criteria of AD that for the first time recognize the unique role of biomarker evidence in disease definition.

Sensitivity and specificity are on the order of 75 to 95%, ***mostly*** around 90% (including in studies with autopsy confirmation)

Key Words: Alzheimer disease; diagnosis; dementia; fluorodeoxyglucose; PET; physician confidence; prognosis

J Nucl Med 2012; 53:59–71

In Canada:

Soucy *et al. Alzheimer's Research & Therapy* 2013, **5(Suppl 1)**:S3
http://alzres.com/content/5/S1/S3

alzheimer's research&therapy

REVIEW

Clinical applications of neuroimaging in patients with Alzheimer's disease: a review from the Fourth Canadian Consensus Conference on the Diagnosis and Treatment of Dementia 2012

Jean-Paul Soucy*[1], Robert Bartha[2], Christian Bocti[3], Michael Borrie[4], Amer M Burhan[4], Robert Laforce Jr[5] and Pedro Rosa-Neto[6]

4th Canadian Consensus Conference on the Diagnosis and Treatment of Dementia

S. Gauthier, C. Patterson, H. Chertkow, M. Gordon, N. Herrmann, K. Rockwood, P. Rosa-Neto, J.P. Soucy on behalf of the CCCDTD4 participants.*

Can J Neurol Sci. 2012;39: Suppl 5: S1-S8

2012
CONFÉRENCE CANADIENNE
CONSENSUELLE SUR LA DÉMENCE

2012
CANADIAN CONSENSUS
CONFERENCE ON DEMENTIA

Neuroimaging - Introduction

For a patient with a diagnosis of dementia who has undergone the recommended baseline clinical and structural brain imaging evaluation and who has been evaluated by a dementia specialist but whose underlying pathological process is still unclear, preventing adequate clinical management, we recommend that the specialist obtain a 18F-FDG PET scan for differential diagnosis purposes (Grade 1B).

Agree

All

Neuroimaging - Introduction

For a patient with MCI evaluated by a dementia specialist and in whom clinical management would be influenced by evidence of an underlying neurodegenerative process, we suggest that an 18F-FDG PET scan be performed or, if not available, than that a SPECT rCBF study be performed (Grade 2C).

Agree

All except 4, one abstention

The diagnosis of dementia due to Alzheimer's disease: Recommendations from the National Institute on Aging-Alzheimer's Association workgroups on diagnostic guidelines for Alzheimer's disease

The diagnosis of mild cognitive impairment due to Alzheimer's disease: Recommendations from the National Institute on Aging-Alzheimer's Association workgroups on diagnostic guidelines for Alzheimer's disease

Alzheimer's & Dementia 7 (2011) 270–279

Marilyn S. Albert[a,*], Steven T. DeKosky[b,c], Dennis Dickson[d], Bruno Dubois[e], Howard H. Feldman[f], Nick C. Fox[g], Anthony Gamst[h], David M. Holtzman[i,j], William J. Jagust[k], Ronald C. Petersen[l], Peter J. Snyder[m,n], Maria C. Carrillo[o], Bill Thies[o], Creighton H. Phelps[p]
Reisa A. Sperling[c], Maria C. Carrillo[o], Bill Thies[o], Creighton H. Phelps[o]

[a]Department of Radiology, Mayo Clinic, Rochester, MN, USA

MCI criteria incorporating biomarkers

Diagnostic category	Biomarker probability of AD etiology	Aβ (PET or CSF)	Neuronal injury (tau, FDG, sMRI)
MCI–core clinical criteria	Uninformative	Conflicting/indeterminant/untested	Conflicting/indeterminant/untested
MCI due to AD—intermediate likelihood	Intermediate	Positive	Untested
		Untested	Positive
MCI due to AD—high likelihood	Highest	Positive	Positive
MCI—unlikely due to AD	Lowest	Negative	Negative
With evidence of AD pathophysiological process	High but does not rule out second etiology	Positive or indeterminate	Positive or indeterminate
Dementia-unlikely due to AD	Lowest	Negative	Negative

Harmonized diagnostic criteria for Alzheimer's disease: recommendations

Journal of Internal Medicine, 2014, 275; 204–213

J. C. Morris[1], K. Blennow[2], L. Froelich[3], A. Nordberg[4], H. Soininen[5,6], G. Waldemar[7], L.-O. Wahlund[8] & B. Dubois[9,10]

The neurodegeneration that characterizes AD is initially manifested by decreased neuronal function and ultimately leads to synaptic loss and neuronal death. Neuroimaging can thus identify downstream biomarkers of AD that measure neuronal dysfunction and brain atrophy, particularly in brain regions that are the most vulnerable to the pathophysiological process. The most commonly used degeneration (also known as injury or topographical) biomarkers are medial temporal lobe atrophy and reduced glucose metabolism in temporoparietal regions, as determined by structural magnetic resonance imaging (MRI) and fluorodeoxyglucose (FDG) PET, respectively. Other potential MRI-derived degeneration biomarkers include cerebral cortical thinning [16] and resting state functional connectivity [17], and additional PET-derived measures include changes in regional cerebral blood flow [18]. Degeneration biomarkers are less specific for AD than molecular biomarkers.

EFNS task force: the use of neuroimaging in the diagnosis of dementia

M. Filippi[a], F. Agosta[a], F. Barkhof[b], B. Dubois[c], N. C. Fox[d], G. B. Frisoni[e], C. R. Jack[f], P. Johannsen[g], B. L. Miller[h], P. J. Nestor[i], P. Scheltens[j], S. Sorbi[k], S. Teipel[l], P. M. Thompson[m] and L.-O. Wahlund[n]

European Journal of Neurology 2012, **19:** 1487–1511

Recommendations for functional imaging

1 Although typical cases of dementia may not benefit from routine SPECT or PET imaging, these tools are recommended in those cases where diagnosis remains in doubt after clinical and structural MRI work-up and in particular clinical settings (class II, level A).

2 Functional imaging can be of value to diagnose (or exclude) a neurodegenerative dementia in those subjects with cognitive impairment presenting with severe psychiatric disturbances (including depression and agitation) and in cases where proper cognitive testing is difficult, that is, with no language in common with the clinician (good practice point).

3 Normal FDG PET scan findings, in the presence of the suspicion of dementia, make a neurodegenerative diagnosis less likely (class II, level A).

4 The overall regional pattern of metabolic impairment of the posterior cingulate/precuneus and lateral temporoparietal cortices, more accentuated than frontal cortex deficits, together with the relative preservation of the primary sensorimotor and visual cortices, basal ganglia and cerebellum defines the distinct metabolic phenotype of AD (class II, level A).

5 AD-like metabolic patterns in patients with MCI are predictive of conversion to AD within several years (class II, level A).

6 Occipital hypometabolism, particularly in the primary visual cortex, may be more common in DLB than AD on a group basis (class II, level B). However, on individual scans, the appearances of DLB and AD can be identical. Moreover, occipital hypometabolism is not a specific marker for DLB and can be associated with AD (good practice point).

7 Although an overlap of functional abnormalities between FTD and AD has been shown to occur, the presence of posterior temporal and parietal brain hypoperfusion or hypometabolism is predictive of a pathological diagnosis of AD, whereas a disproportionate reduction in frontal perfusion/metabolism is more common in FTD cases (class II, level A).

^{18}F-FDG PET and Perfusion SPECT in the Diagnosis of Alzheimer and Lewy Body Dementias

J Nucl Med 2014; 55:1959–1965

John T. O'Brien[1,2], Michael J. Firbank[2,3], Christopher Davison[2], Nicky Barnett[2], Claire Bamford[4], Cam Donaldson[4,5], Kirsty Olsen[2], Karl Herholz[6], David Williams[2], and Jim Lloyd[3]

PET *vs* SPECT

CONCLUSION

We undertook a direct comparison of the diagnostic value of ^{18}F-FDG PET and perfusion (HMPAO) SPECT in the differential diagnosis of degenerative dementia and found ^{18}F-FDG PET to be significantly superior to SPECT using all methods of analysis. The performance of SPECT was such that it is of only limited diagnostic value. Although we can envisage circumstances when HMPAO SPECT may still be a useful investigation, in most circumstances and especially when both ^{18}F-FDG PET and perfusion SPECT are available, our results strongly indicate that ^{18}F-FDG PET should be the clinical investigation of choice for the differential diagnosis of degenerative dementia. We recommend that national and international guidelines are updated to reflect this new evidence.

Clinical validity of brain fluorodeoxyglucose positron emission tomography as a biomarker for Alzheimer's disease in the context of a structured 5-phase development framework

Valentina Garibotto [a,*], Karl Herholz [b], Marina Boccardi [c,d], Agnese Picco [d,e], Andrea Varrone [f], Agneta Nordberg [g], Flavio Nobili [e], Osman Ratib [a], for the Geneva Task Force for the Roadmap of Alzheimer's Biomarkers

Neurobiology of Aging 52 (2017) 183–195

ABSTRACT

The use of Alzheimer's disease (AD) biomarkers is supported in diagnostic criteria, but their maturity for clinical routine is still debated. Here, we evaluate brain fluorodeoxyglucose positron emission tomography (FDG PET), a measure of cerebral glucose metabolism, as a biomarker to identify clinical and prodromal AD according to the framework suggested for biomarkers in oncology, using homogenous criteria with other biomarkers addressed in parallel reviews.

aims.

. The results of this study show that specific efforts are needed to complete phase 3 evidence, in particular comparing and combining FDG PET with other biomarkers, and to properly design phase 4 prospective studies as a basis for phase 5 evaluations.

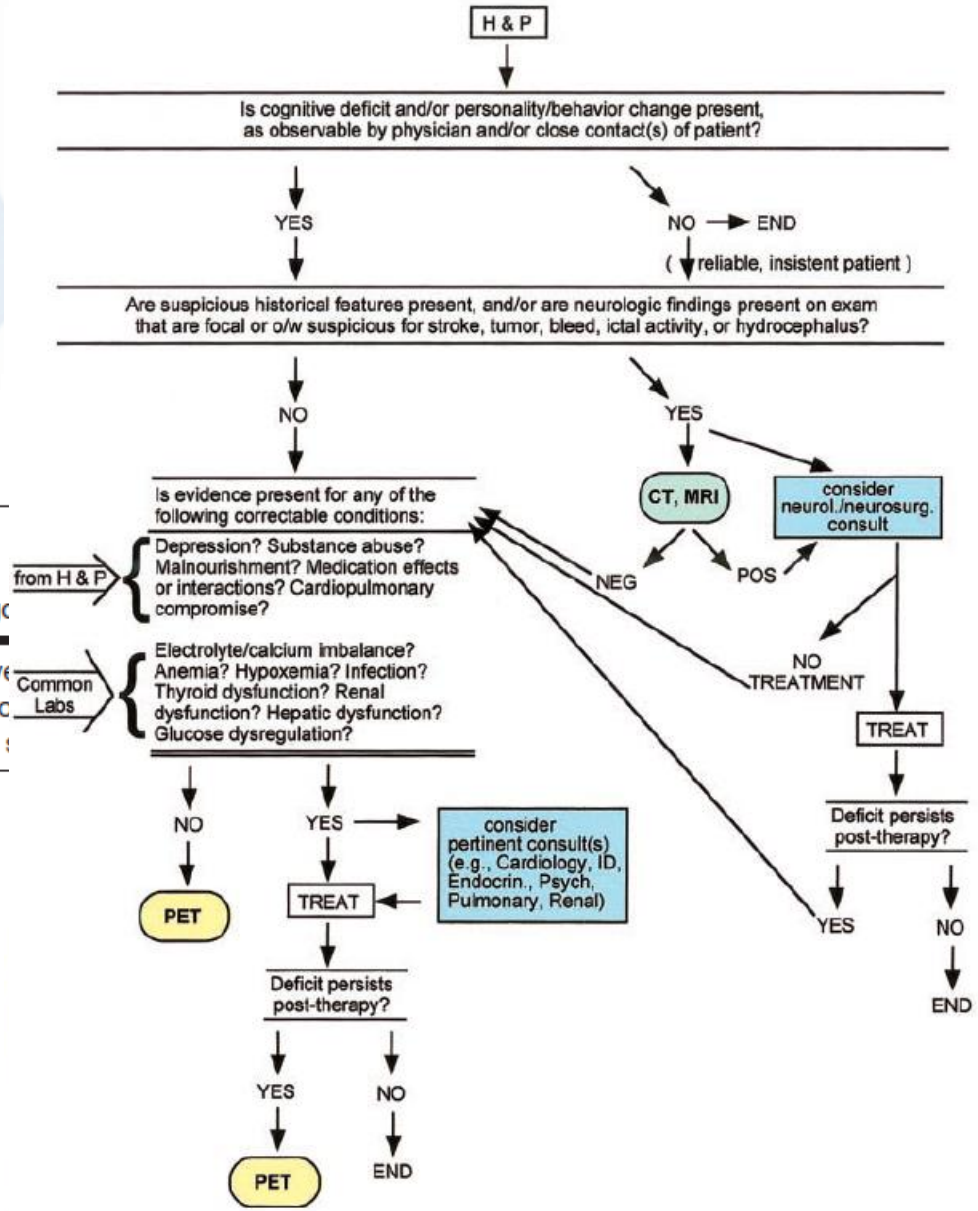

FIGURE 2. Proposed guidelines for determining when to obtain brain PET study in evaluation of geriatric patients with early symptoms of cognitive decline. H & P = history and physical examination; exam = examination; o/w = otherwise; bleed = bleeding; neurol. = neurologic; neurosurg. = neurosurgical; consult = consultation; NEG = negative; POS = positive; Labs = laboratory tests; ID = infectious disease; Endocrin. = endocrinology; Psych = psychology.

Cost-effectiveness of ^{18}F-fluorodeoxyglucose positron emission tomography in the assessment of early dementia from a Belgian and European perspective

G. Moulin-Romsee[a], A. Maes[a], D. Silverman[b], L. Mortelmans[a] and K. Van Laere[a]

Early identification and treatment of Alzheimer's disease: Social and fiscal outcomes

Alzheimer's & Dementia 5 (2009) 215–226

David L. Weimer[a], Mark A. Sager[b,*]

Clinical and cost effectiveness of services for early diagnosis and intervention in dementia

Int J Geriatr Psychiatry 2009; **24**: 748–754

Sube Banerjee[1*] and Raphael Wittenberg[2]

An economic evaluation of early assessment for Alzheimer's disease in the United Kingdom

Alzheimer's & Dementia 8 (2012) 22–30

Dennis Getsios[a,*], Steve Blume[b], Khajak J. Ishak[c], Grant Maclaine[d], Luis Hernández[e,f]

Medical costs of Alzheimer's disease misdiagnosis among US Medicare beneficiaries

Alzheimer's & Dementia 11 (2015) 887-895

Craig A. Hunter[a], Noam Y. Kirson[b,*], Urvi Desai[b], Alice Kate G. Cummings[b], Douglas E. Faries[a], Howard G. Birnbaum[b]

Still, those studies remain complex …

Diagnosing Alzheimer's disease: A systematic review of economic evaluations

Alzheimer's & Dementia 10 (2014) 225–237

Ron L. H. Handels[a,*], Claire A. G. Wolfs[a], Pauline Aalten[a], Manuela A. Joore[b], Frans R. J. Verhey[a], Johan L. Severens[c]

We focused on the diagnostic aspects of the decision models to assess the applicability of existing decision models for the evaluation of the recently revised diagnostic research criteria for AD.

Methods: PubMed and the National Institute for Health Research Economic Evaluation database were searched for English-language publications related to economic evaluations on diagnostic technologies. Trial-based economic evaluations were assessed using the Consensus on Health Economic Criteria list. Modeling studies were assessed using the framework for quality assessment of decision-analytic models.

Results: The search retrieved 2109 items, from which

. Recommendations were focused on diagnostic aspects and the applicability of existing models for the evaluation of recently revised diagnostic research criteria for AD.

But they all showed significant savings when ^{18}FDG PET is performed early!!!

Document Title Models of Dementia Assessment and Diagnosis: Indicative Cost Review

Version number: 1

First published: September 2015

Prepared by: NHS England

Classification: OFFICIAL

Models of Dementia Assessment and Diagnosis: Indicative Cost Review

Northumberland, Tyne and Wear NHS Foundation Trust Pathway

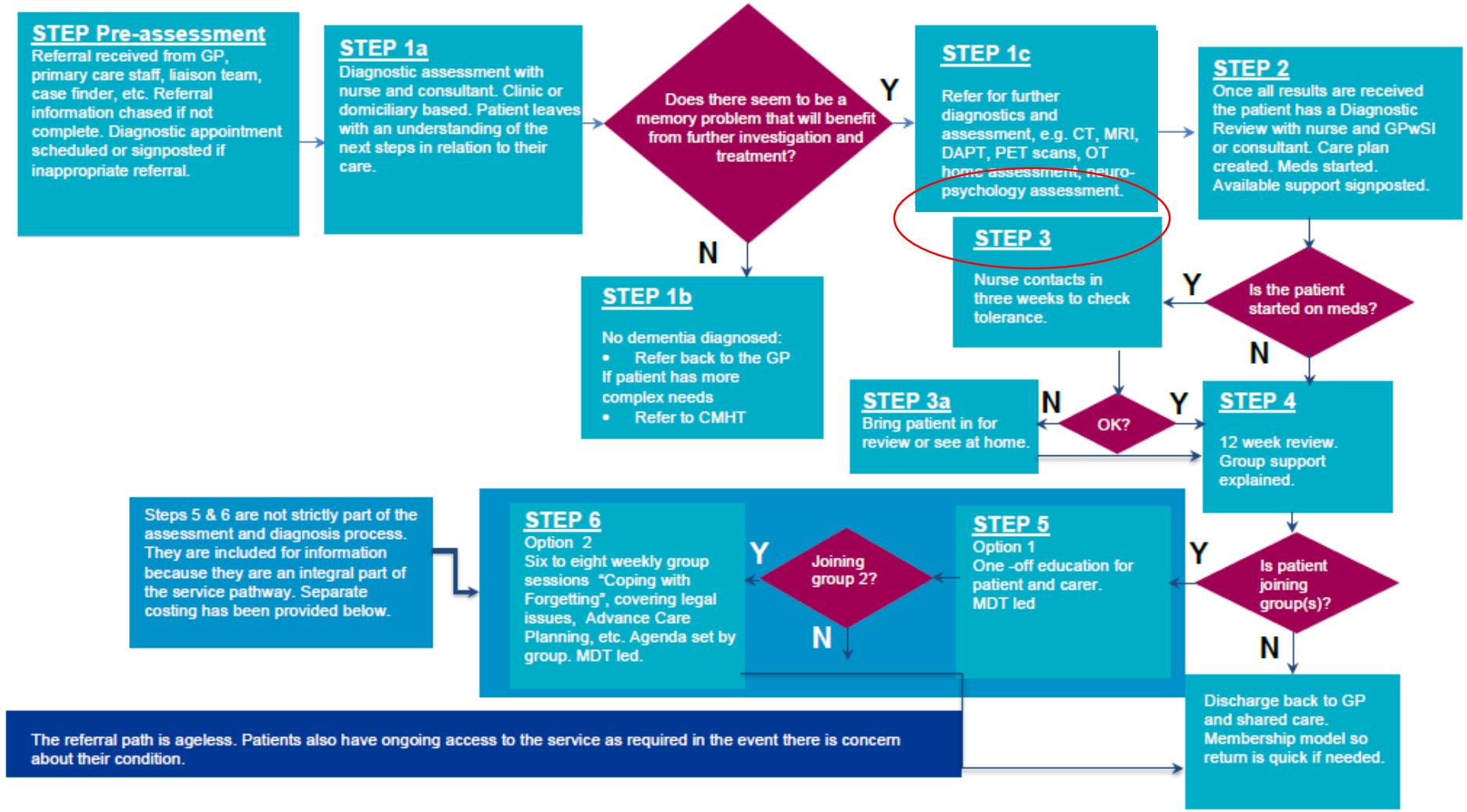

And for a really up-to-date review of ^{18}FDG PET:

Review Article

Molecular imaging in dementia: Past, present, and future

R. Laforce, Jr.[a,*], J. P. Soucy[b], L. Sellami[a], C. Dallaire-Théroux[a], F. Brunet[a], D. Bergeron[a], B. L. Miller[c], R. Ossenkoppele[d]

Alzheimer's & Dementia ■ (2018) 1-31

2.3.1.1. Atypical complex cases with an uncertain diagnosis

Diagnosis of neurodegenerative diseases can be challenging, particularly in the early stages of the disease, in younger patients, in atypical/unclear presentations, or in patients with comorbid neuropsychiatric symptomatology [63–65]. Delay in treatment due to diagnostic uncertainty, particularly frequent in atypical/unclear degenerative diseases, has important clinical and psychological consequences for patients and their families [66,67]. In tertiary care memory clinics, where the most complex patients are seen, a significant proportion of cases remain unclear despite a comprehensive clinical evaluation. For such atypical/unclear degenerative diseases, further investigation is often undertaken to obtain a clear diagnosis. These complementary evaluations include a detailed neuropsychological evaluation, blood tests, CSF analysis, MRI, and molecular imaging with FDG-PET. A growing body of evidence indeed supports the value of FDG-PET in the diagnosis of patients with atypical/unclear conditions [24,32,35,68–73]. Importantly, FDG-PET can improve diagnostic accuracy and lead to earlier treatment, better planning for future care, and less suffering for patients and their families. In 2010, a retrospective memory clinic study evaluating

My opinion (based on over 9000 cases) on what is ***generally*** justified?

- Diagnostic needs to be specified in order to determine therapy go/no-go (disease-appropriate, tolerable side effects, cost)
- Prognosis (personal/familial), in cases of minor or major NCD of unknown etiology
- Prognosis in cases of subjective NCD in patients with a positive family history of neurodegenerative disease, faced with professional or life-style altering decisions
- Any case where a consultant can convince me that, although unusual, the reason for the test is indeed valid

P.S.: one ^{18}FDG dose in Quebec? From a few $100s to next to nothing…

Plan/Objectives

- The established:
  ^{18}F-FDG: old, but still going strong!/ A quick, brief, not long, short discussion to remember that it's still the best we have

- The almost there:
  - Amyloid PET Imaging: good, work-in-progress/ Understand what it means to find plaques in the brain in order to define clinical indications
  - Tau imaging/ Recognize that it's great for research, and might also be for patients

- The future / Review some avenues that will keep us relevant

Amyloid ligands

It took a few decades,
but finally …

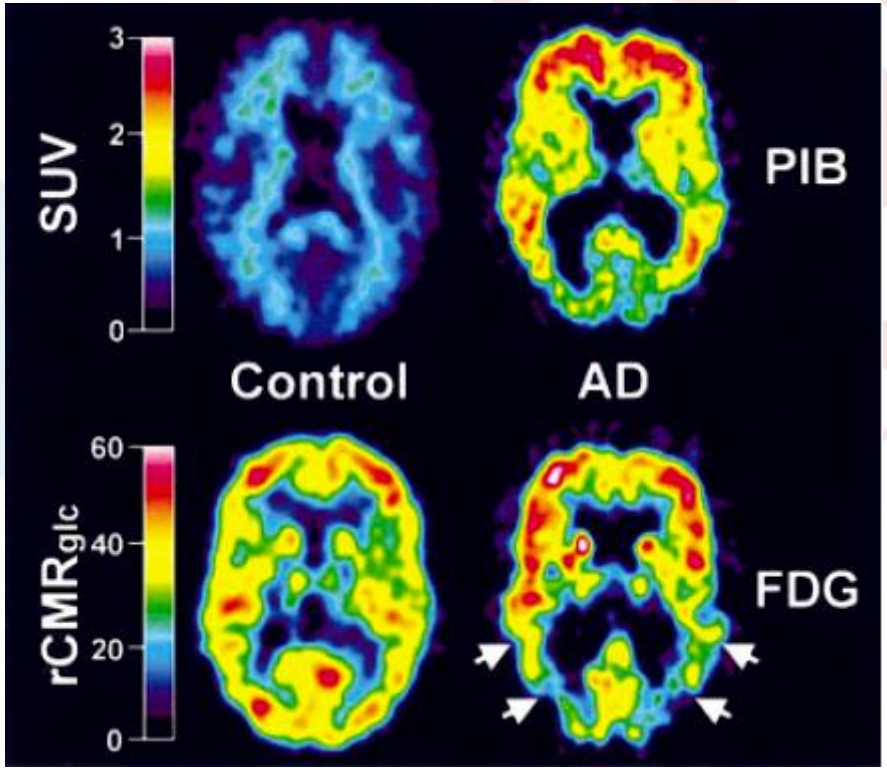

Imaging Brain Amyloid in Alzheimer's Disease with Pittsburgh Compound-B

Ann Neurol 2004;55:306–319

William E. Klunk, MD, PhD,[1] Henry Engler, MD,[2] Agneta Nordberg, MD, PhD,[3,4] Yanming Wang, PhD,[5] Gunnar Blomqvist, PhD,[2] Daniel P. Holt, BS,[5] Mats Bergström, PhD,[2] Irina Savitcheva, MD,[2] Guo-feng Huang, PhD,[5] Sergio Estrada, PhD,[2] Birgitta Ausén, MSCI,[4] Manik L. Debnath, MS,[1] Julien Barletta, BS,[6] Julie C. Price, PhD,[5] Johan Sandell, PhD,[2] Brian J. Lopresti, BS,[5] Anders Wall, PhD,[2] Pernilla Koivisto, PhD,[2] Gunnar Antoni, PhD,[2] Chester A. Mathis, PhD,[5] and Bengt Långström, PhD[2,6]

And so logically too... binding to ...

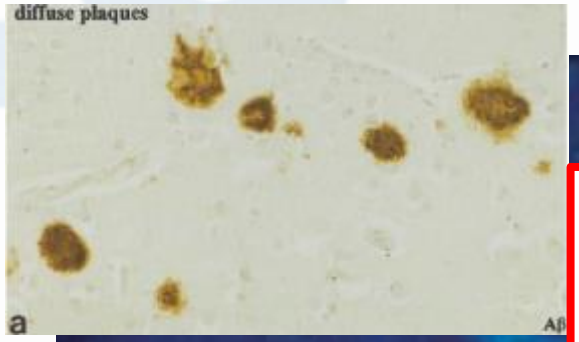

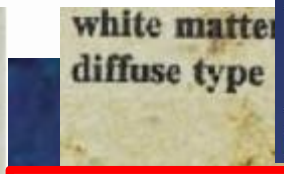

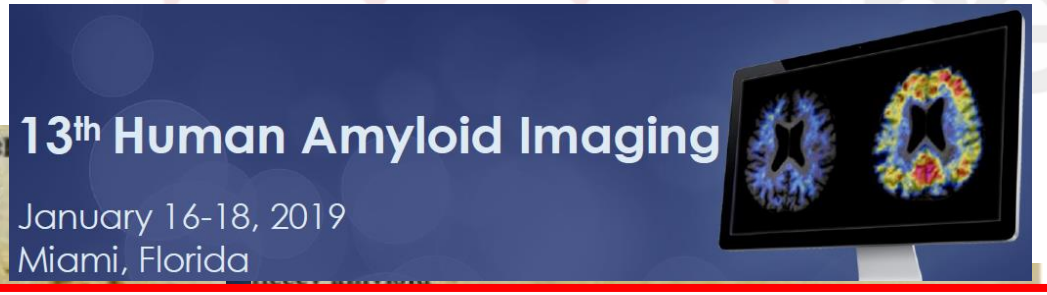

Postmortem analyses of PiB and Flutemetamol integrated density measures in diffuse and neuritic plaques in Alzheimer's disease

Milos Ikonomovic[1], Chris Buckley[2], Eric Abrahamson[1], Chester Mathis[1], William Klunk[1], Gill Farrar[2]

Discussion: [C-11]PiB and [F-18]Flutemetamol PET retention in vivo likely depends on both the size and fibrillar density of plaques in brain regions analyzed. In two brain regions with similar total plaque burden, the region with predominant NPs yields higher integrated density values. However, large swaths of DPs could yield PET ligands' retention levels similar to those detected in the much smaller volumes of NPs. Thus, amyloid PET may correlate better with NIA-AA 2012 AD neuropathology criteria that incorporate both CERAD (NP) and Thal phases (all types of Aβ plaques).

(nor to βA oligomers, NFTs or other tau species, Lewy bodies, etc.)

↓

THOSE, NOT PLAQUES, are the toxic entities in AD!!!

Amyloid ligands labeled with [^{18}F]

So far the best, but …

	[^{11}C]PIB	[^{18}F]Flutemetamol	[^{18}F]Florpetabir	[^{18}F]Florbetaben	[^{18}F]NAV4694
	Research	**Approved UE/FDA**	**Approved UE/FDA**	**Approved UE/FDA** And Canada!!	**Phase 2**
Other name		GE-067	AV45 / AMIVID	BAY-94-9172, AV-1	**[^{18}F]NAV4694**
Class	Benzothiazole	Benzothiazole	Styrylpyridine	Stilbene	Benzothiazole
Affinity βA (Ki, nM)	0.9	0.7	2.2.	2.4	0.7
Metabolites in Plasma	Polar	Polar	Polar and non-polar	Polar and non-polar	Polar
Typical Inject. Act. (MBq)	250–450	250–450	300	300	300
Post IV Imaging (min)	40–90	80–100	50–70	90–130	50-60
Structure	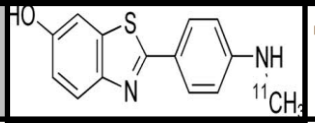	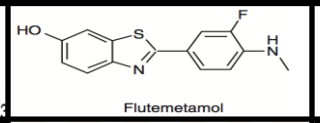	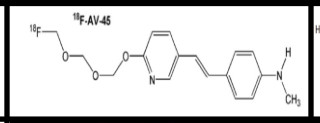	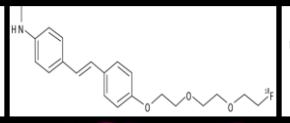	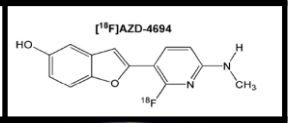
AD examples	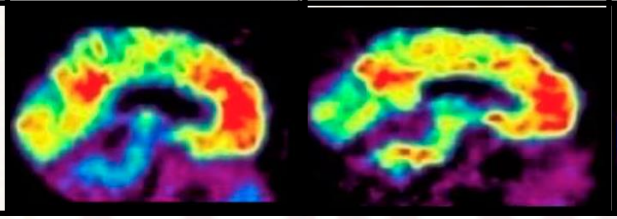			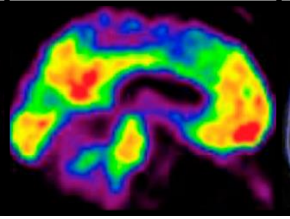	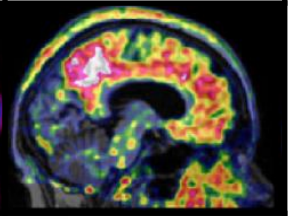

Adapted from Herholz, Lancet Neurol 2011; 10: 667–70

Diagnostic accuracy of ^{18}F amyloid PET tracers for the diagnosis of Alzheimer's disease: a systematic review and meta-analysis

Elizabeth Morris[1,2] · Anastasia Chalkidou[1,2] · Alexander Hammers[2] · Janet Peacock[1,3,4] · Jennifer Summers[1,3,4] · Stephen Keevil[1,2,5]

Eur J Nucl Med Mol Imaging (2016) 43:374–385

Abstract Imaging or tissue biomarker evidence has been introduced into the core diagnostic pathway for Alzheimer's disease (AD). PET using ^{18}F-labelled beta-amyloid PET tracers has shown promise for the early diagnosis of AD. However, most studies included only small numbers of participants and no consensus has been reached as to which radiotracer has the highest diagnostic accuracy. First, we performed a systematic review of the literature published between 1990 and 2014 for studies exploring the diagnostic accuracy of florbetaben, florbetapir and flutemetamol in AD. The included studies were analysed using the QUADAS assessment of methodological quality. A meta-analysis of the sensitivity and specificity reported within each study was performed. Pooled values were calculated for each radiotracer and for visual or quantitative analysis by population included. The systematic review identified nine studies eligible for inclusion. There were limited variations in the methods between studies reporting the same radiotracer. The meta-analysis results showed that pooled sensitivity and specificity values were in general high for all tracers. This was confirmed by calculating likelihood ratios. A patient with a positive ratio is much more likely to have AD than a patient with a negative ratio, and vice versa. However, specificity was higher when only patients with AD were compared with healthy controls. This systematic review and meta-analysis found . All tracers perform better when used to discriminate between patients with AD and healthy controls. The sensitivity and specificity for quantitative and visual analysis are comparable to those of other imaging or biomarker techniques used to diagnose AD. Further research is required to identify the combination of tests that provides the highest sensitivity and specificity, and to identify the most suitable position for the tracer in the clinical pathway.

3.4 Image Display and Interpretation

images should be interpreted only by readers who successfully complete Electronic Media- or In-Person Training provided by the manufacturer [see Warnings and Precautions (5.1)]. The objective of florbetaben F 18 image interpretation is to estimate β-amyloid neuritic plaque density in brain gray matter, not to make a clinical diagnosis. Image interpretation is performed independently of a patient's clinical features and relies upon the recognition of image features in certain brain regions.

Image Display

PET images should be displayed in the transaxial orientation using gray scale or inverse gray scale. The sagittal and coronal planes may be used for additional orientation purposes. CT or MR images may be helpful for anatomic reference purposes. However, visual assessment should be performed using the axial planes according to the recommended reading methodology.

Image Interpretation

Regions displayed in the PET images which 'anatomically' correspond to white matter structures (e.g., the cerebellar white matter or the splenium) should be identified to help the readers orient themselves. Images should be viewed and assessed in a systematic manner, starting with the cerebellum and scrolling up through the lateral temporal and frontal lobes, the posterior cingulate cortex/precuneus, and the parietal lobes. For a gray matter cortical region to be assessed as showing 'tracer uptake', the majority of slices from the respective region must be affected.

For each patient, the This determination is based on the assessment of tracer uptake in the gray matter of the following four brain regions: the temporal lobes, the frontal lobes, the posterior cingulate cortex/precuneus, and the parietal lobes; according to the following 'rules for assessment' [see Warnings and Precautions (5.1.)]:

National Institute on Aging–Alzheimer's Association guidelines for the neuropathologic assessment of Alzheimer's disease: a practical approach

Acta Neuropathol (2012) 123:1–11

Thomas J. Montine · Creighton H. Phelps · Thomas G. Beach · Eileen H. Bigio · Nigel J. Cairns · Dennis W. Dickson · Charles Duyckaerts · Matthew P. Frosch · Eliezer Masliah · Suzanne S. Mirra · Peter T. Nelson · Julie A. Schneider · Dietmar Rudolf Thal · John Q. Trojanowski · Harry V. Vinters · Bradley T. Hyman

AD neuropathologic change		B[a]		
A[b]	C[c]	0 or 1	2	3
0	0	Not[d]	Not[d]	Not[d]
1	0 or 1	Low	Low	Low[e]
	2 or 3[f]	Low	Intermediate	Intermediate[e]
2	Any C	Low[g]	Intermediate	Intermediate[e]
3	0 or 1	Low[g]	Intermediate	Intermediate[e]
	2 or 3	Low[g]	Intermediate	High

AD neuropathologic change is evaluated with an "ABC" score (Table 2): Aβ/amyloid plaques (A), NFT stage (B), and neuritic plaque score (C).

Clinicopathologic and ^{11}C-Pittsburgh compound B implications of Thal amyloid phase across the Alzheimer's disease spectrum

Melissa E. Murray,[1] Val J. Lowe,[2] Neill R. Graff-Radford,[3] Amanda M. Liesinger,[1] Ashley Cannon,[1] Scott A. Przybelski,[4] Bhupendra Rawal,[5] Joseph E. Parisi,[6] Ronald C. Petersen,[7] Kejal Kantarci,[2] Owen A. Ross,[1] Ranjan Duara,[8] David S. Knopman,[7] Clifford R. Jack Jr.[2] and Dennis W. Dickson[1]

BRAIN 2015: 138; 1370–1381

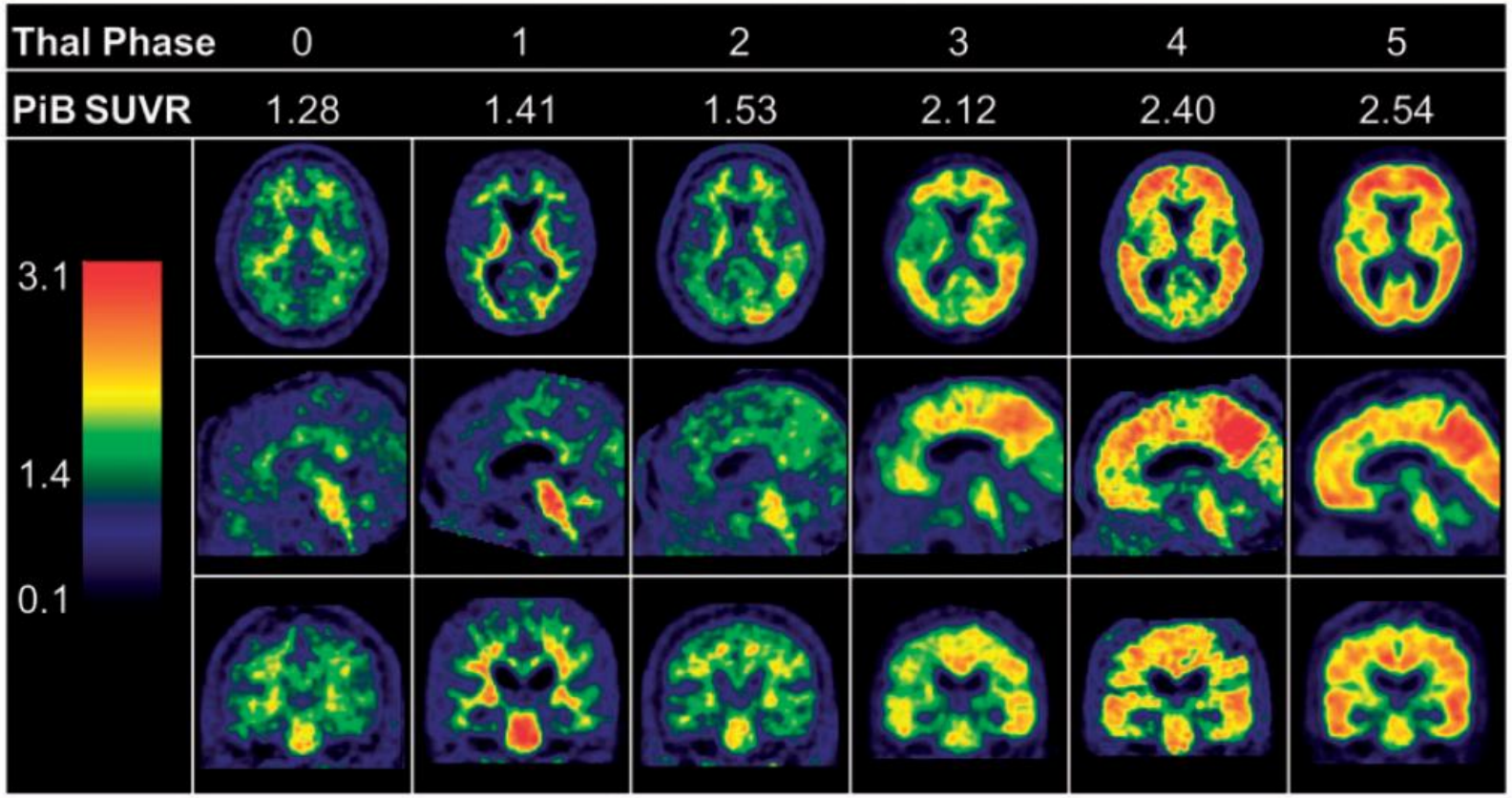

Figure 3 Comparison of ^{11}C-PiB SUV ratio images across each Thal amyloid phase. The PiB-PET SUV ratio values can be found below each Thal amyloid phase. Representative axial, sagittal, and coronal slices from PiB-PET of six Mayo Clinic Rochester participants' shows increasing PiB-positivity with each subsequent Thal amyloid phase. All example images are spatially and intensity normalized. The heat map index (*left*) shows the start of green at a SUV ratio level of 1.4, which is the cut-off point used to assess PiB-positivity. Of note, cerebellar PiB-PET uptake in Thal amyloid Phase 5 is not visible as this is the region used to normalize the scan. SUVR = SUV ratio.

National Institute on Aging–Alzheimer's Association guidelines for the neuropathologic assessment of Alzheimer's disease: a practical approach

Acta Neuropathol (2012) 123:1–11

Thomas J. Montine · Creighton H. Phelps · Thomas G. Beach · Eileen H. Bigio · Nigel J. Cairns · Dennis W. Dickson · Charles Duyckaerts · Matthew P. Frosch · Eliezer Masliah · Suzanne S. Mirra · Peter T. Nelson · Julie A. Schneider · Dietmar Rudolf Thal · John Q. Trojanowski · Harry V. Vinters · Bradley T. Hyman

AD neuropathologic change		B[a]		
A[b]	C[c]	0 or 1	2	3
0	0	Not[d]	Not[d]	Not[d]
1	0 or 1	Low	Low	Low[e]
	2 or 3[f]	Low	Intermediate	Intermediate[e]
2	Any C	Low[g]	Intermediate	Intermediate[e]
3	0 or 1	Low[g]	Intermediate	Intermediate[e]
	2 or 3	Low[g]	Intermediate	High

Passage to "significant" levels

AD neuropathologic change is evaluated with an "ABC" score (Table 2): Aβ/amyloid plaques (A), NFT stage (B), and neuritic plaque score (C).

Florbetaben PET imaging to detect amyloid beta plaques in Alzheimer's disease: Phase 3 study

Alzheimer's & Dementia 11 (2015) 964-974

Osama Sabri[a,*,1], Marwan N. Sabbagh[b,1], John Seibyl[c], Henryk Barthel[a], Hiroyasu Akatsu[d,e,f], Yasuomi Ouchi[g], Kohei Senda[h], Shigeo Murayama[i,j], Kenji Ishii[j], Masaki Takao[j,k], Thomas G. Beach[b], Christopher C. Rowe[l], James B. Leverenz[m,3], Bernardino Ghetti[n], James W. Ironside[o], Ana M. Catafau[p], Andrew W. Stephens[p], Andre Mueller[p], Norman Koglin[p], Anja Hoffmann[q], Katrin Roth[q], Cornelia Reininger[q,1], Walter J. Schulz-Schaeffer[r,1], and for the Florbetaben Phase 3 Study Group[2]

Background: Evaluation o…ography (PET) imaging can assist in the diagnosis of Al…

Methods: Open-label, nonr…idate the ^{18}F-labeled β-amyloid tracer florbetaben by …ortem histopathology.

Results: …participants) were analyzed. …In a subgroup, a regional tissue-scan matched analysis was performed. In areas known to strongly accumulate β-amyloid plaques, sensitivity and specificity were 82% to 90%, and 86% to 95%, respectively.

Conclusions: Florbetaben PET shows high sensitivity and specificity for the detection of histopathology-confirmed neuritic β-amyloid plaques and may thus be a valuable adjunct to clinical diagnosis, particularly for the exclusion of AD.

- Amyloid Imaging

(give or take 2%…) =

No AD

So, that's good. But we really need more to have a home run …

HIGH LIGHT

Cortical biochemistry in MCI and Alzheimer disease

Lack of correlation with clinical diagnosis

M.S. Forman, MD, PhD; E.J. Mufson, PhD; S. Leurgans, PhD; D. Pratico, MD; S. Joyce, BS; S. Leight, BS; V.M.-Y. Lee, PhD; and J.Q. Trojanowski, MD, PhD

Abstract—*Objective:* Mild cognitive impairment, hypothesized to be prodromal Alzheimer disease (AD), shows abundant senile plaques and neurofibrillary tangles, but its biochemical correlates remain undefined. *Methods:* in postmortem frozen brains from subjects diagnosed antemortem with no cognitive impairment, mild cognitive impairment, or AD. *Results:* , but insoluble Aβ and 8,12-iso-iPF$_{2\alpha}$-VI levels from gray matter of all brain regions correlated strongly with the burden of AD pathology, whereas insoluble tau did not. *Conclusions:* The biochemical alterations in cortical tau, Aβ, and isoprostane do not reflect the onset of clinical dementia.

NEUROLOGY 2007;68:757–763

10 NCI, 10 MiCI, 10 MaCI AD, Religious Order Study

Prevalence of Cerebral Amyloid Pathology in Persons Without Dementia
A Meta-analysis

Willemijn J. Jansen, MSc; Rik Ossenkoppele, PhD; Philip Scheltens, MD, PhD; Frans R. J. Verhey, MD; and the Amyloid Biomarker Study Group

Figure 2. Association of Age With Positivity According to Cognitive

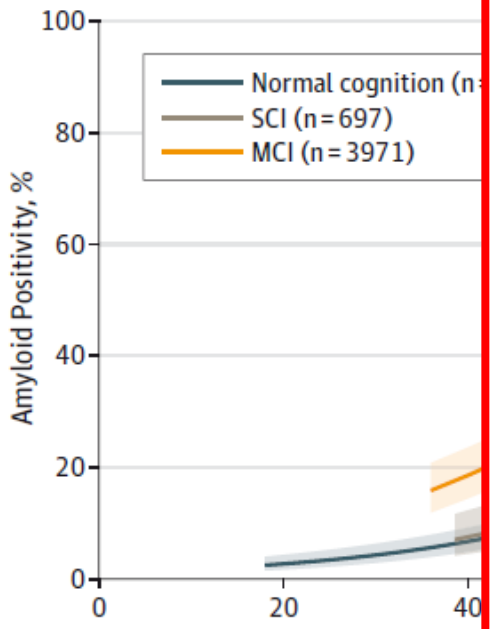

The prevalence estimates were generated from generalized estimating equations. The model included age and cognitive status as predictors. Shading indicates 95% CIs; SCI, subjective cognitive impairment; MCI, mild cognitive impairment.

Prevalence of Amyloid PET Positivity in Dementia Syndromes
A Meta-analysis

JAMA. 2015;313(19):1939-1949

Rik Ossenkoppele, PhD; Willemijn J. Jansen, MSc; Gil D. Rabinovici, MD; Dirk L. Knol, PhD; Wiesje M. van der Flier, PhD; Bart N. M. van Berckel, MD, PhD;

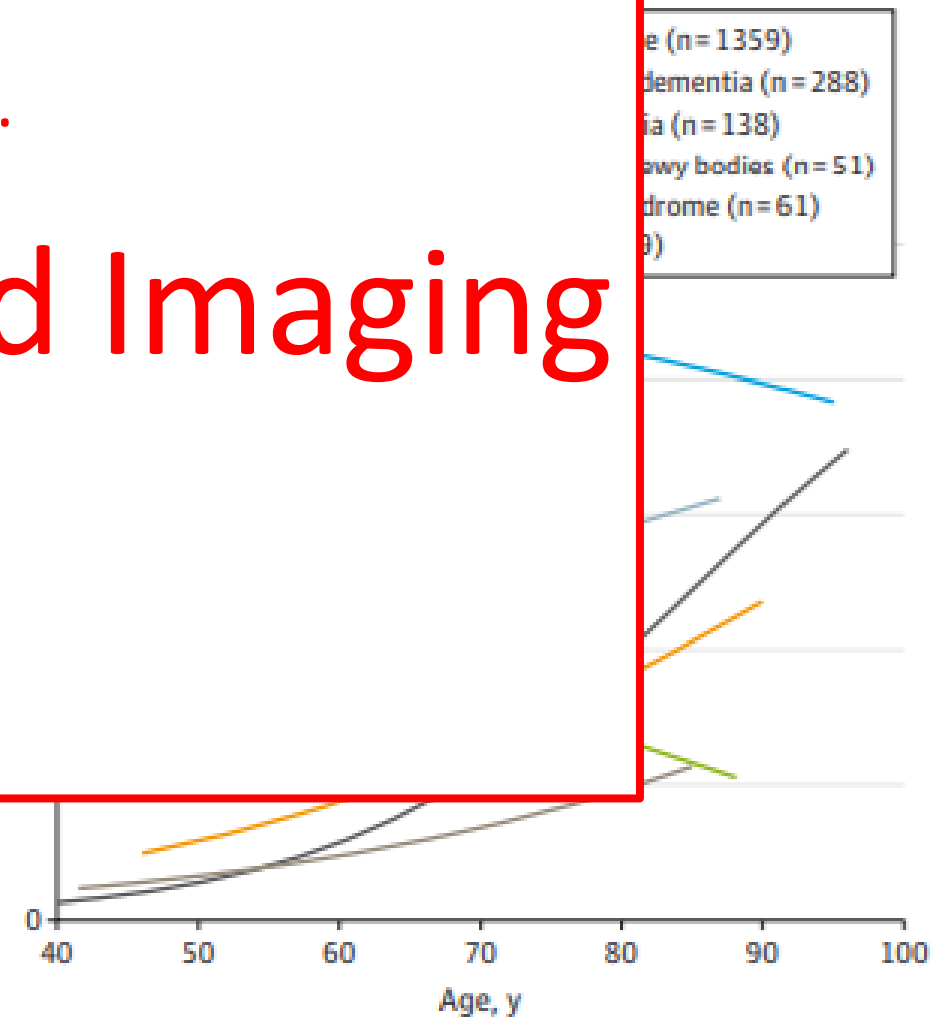

- Amyloid Imaging

=

No AD …

But + Amyloid Imaging

So, mixed results …

≠

AD

Appropriate Use Criteria for Amyloid PET: A Report of the Amyloid Imaging Task Force, the Society of Nuclear Medicine and Molecular Imaging, and the Alzheimer's Association

J Nucl Med 2013; 54:476–490

Keith A. Johnson[1], Satoshi Minoshima[2], Nicolaas I. Bohnen[3], Kevin J. Donohoe[4], Norman L. Foster[5], Peter Herscovitch[6], Jason H. Karlawish[7], Christopher C. Rowe[8], Maria C. Carrillo[9], Dean M. Hartley[9], Saima Hedrick[10], Virginia Pappas[10], and William H. Thies[9]

Amyloid imaging is appropriate in the situations listed here for individuals with all of the following characteristics:

Preamble: (*i*) a cognitive complaint with objectively confirmed impairment; (*ii*) AD as a possible diagnosis, but when the diagnosis is uncertain after a comprehensive evaluation by a dementia expert; and (*iii*) when knowledge of the presence or absence of Aβ pathology is expected to increase diagnostic certainty and alter management.

1. Patients with persistent or progressive unexplained MCI
2. Patients satisfying core clinical criteria for possible AD because of unclear clinical presentation, either an atypical clinical course or an etiologically mixed presentation
3. Patients with progressive dementia and atypically early age of onset (usually defined as 65 years or less in age)

AFTER a non-conclusive FDG study!

Update on appropriate use criteria for amyloid PET imaging: Dementia experts, mild cognitive impairment, and education

Alzheimer's & Dementia 9 (2013) e106–e109

Keith A. Johnson[a], Satoshi Minoshima[b], Nicolaas I. Bohnen[c], Kevin J. Donohoe[d], Norman L. Foster[e], Peter Herscovitch[f], Jason H. Karlawish[g], Christopher C. Rowe[h], Saima Hedrick[i], Virginia Pappas[i], Maria C. Carrillo[j,*], Dean M. Hartley[j]

expert. Nevertheless, we concluded that a [redacted] for this purpose should be self-identified as a physician trained and board-certified in neurology, psychiatry, or geriatric medicine who devotes a substantial proportion ($\geq$25%) of patient contact time to the evaluation and care of adults with acquired cognitive impairment or dementia, including probable or suspected Alzheimer disease, as confirmed by peer recognition. Physicians particularly likely to have these

Canadian Consensus Guidelines on Use of Amyloid Imaging in Canada: Update and Future Directions from the Specialized Task Force on Amyloid imaging in Canada

Can J Neurol Sci. 2016; doi:10.1017/cjn.2015.401

BEFORE HC Approval!

Robert Laforce Jr., Pedro Rosa-Neto, Jean-Paul Soucy, Gil D. Rabinovici, Bruno Dubois, S. Gauthier, on behalf of the consensus meeting participants

Table 1: Recommendations for clinicians on behalf of the Canadian Consensus Conference on the Use of Amyloid Imaging

1.	Amyloid imaging represents a promising technique in the evaluation of dementia for which much has been learned over the past decade. It is not currently approved for clinical use in Canada. A. In accord with Appropriate Use Criteria for Amyloid PET,[59,61] we recommend its use in patients with objectively confirmed cognitive impairments in whom there is diagnostic uncertainty* after a comprehensive clinical evaluation (mental status testing, laboratory tests, and structural brain imaging using MRI†), and in whom knowledge of Aβ status is expected to provide a more precise diagnosis and alter management; B. Clinicians who wish to obtain amyloid imaging should refer patients to dementia centers with an expertise in this technique, i.e. dementia experts‡ with substantial clinical experience and practice in dementia care who work in conjunction with nuclear medicine specialists qualified in amyloid imaging; C. We strongly recommend against the use of amyloid imaging in cognitively normal individuals or for the initial investigation of cognitive complaints.
2.	Physicians should be cautious about interpreting the significance of amyloid test results, i.e. used in isolation this test cannot diagnose AD,[6,7] MCI,[8,33,34] or differentiate normal from abnormal aging. When faced with such situations, we recommend they consult with dementia centers with an expertise in this technique.
3.	At present, there is no clinical indication for amyloid imaging in: A. Attempting to differentiate AD from other aβ-associated dementia (e.g. dementia with Lewy bodies, cerebral amyloid angiopathy); B. Attempting to differentiate between AD clinical variants (e.g. classic amnestic AD vs. posterior cortical atrophy or logopenic variant of primary progressive aphasia); C. Attempting to differentiate between the various clinical presentations associated with frontotemporal lobar degeneration spectrum of disorders (e.g. behavioral variant frontotemporal dementia vs progressive supranuclear palsy) to try to define the underlying pathology; D. Staging the severity of a dementing syndrome.
4.	
5.	The actual process of undergoing an amyloid scan and the implications associated with disclosure of the results should be taken very seriously because this can be highly stressful for patients and families. To maximize safety and effectiveness of disclosing results, we recommend adopting parts of the sequence recently developed by Harkins et al[65] in cognitively normal older adults participating in AD prevention studies. This format includes an educational session with clinical scenarios before the scan, assessment of mood and willingness to receive the results, and a formal face-to-face disclosure session in which results are discussed along with their diagnostic and prognostic implications.

Clinical validity of increased cortical uptake of amyloid ligands on PET as a biomarker for Alzheimer's disease in the context of a structured 5-phase development framework

Konstantinos Chiotis [a], Laure Saint-Aubert [a], Marina Boccardi [b,c], Anton Gietl [d], Agnese Picco [e], Andrea Varrone [f], Valentina Garibotto [g], Karl Herholz [h], Flavio Nobili [e], Agneta Nordberg [a,i,*], for the Geneva Task Force for the Roadmap of Alzheimer's Biomarkers[1]

Neurobiology of Aging 52 (2017) 214–227

A B S T R A C T

The use of biomarkers has been proposed for diagnosing Alzheimer's disease in recent criteria, but some biomarkers have not been sufficiently investigated to justify their routine clinical use. Here, we evaluate in a literature review the clinical validity of amyloid positron emission tomography (PET) imaging using a structured framework developed for the assessment of oncological biomarkers. Homogenous criteria have been addressed in reviews of other Alzheimer's disease biomarkers. There is adequate evidence that

while

. This review highlights the priorities to be pursued to enable the proper use of amyloid PET imaging in a clinical setting. Future investigations will primarily be large, phase 4 studies that will assess the utility of amyloid PET imaging in routine clinical practice.

Research!

Clinical!

Gil Rabinovici, MD

IDEAS
Imaging Dementia—Evidence For Amyloid Scanning

WHAT

The Imaging Dementia—Evidence for Amyloid Scanning (IDEAS) Study will determine the clinical usefulness on patient-oriented outcomes of a brain positron emission tomography (PET) scan that detects amyloid plaques, a core feature of Alzheimer's disease. In addition to assessing the impact of amyloid PET on management of patients with mild cognitive impairment or dementia of uncertain cause, the study will compare medical outcomes for study participants with matched patients not in the study.

WHY

By providing access to amyloid imaging for more than 18,000 Medicare beneficiaries for whom there is ambiguity about the cause of their cognitive decline/dementia, the IDEAS Study seeks to demonstrate that amyloid PET can help clinicians diagnose the cause of cognitive impairment, provide the most appropriate treatments and recommendations, and improve health outcomes. It is anticipated that the evidence obtained by the IDEAS Study will support reimbursement of amyloid imaging by Medicare and other third-party payers.

WHO

Patients will be enrolled by qualified, participating dementia specialists and must be a Medicare beneficiary, 65 or older, who meets the appropriate use criteria (AUC) for amyloid PET imaging. Amyloid PET may have greatest value in patients with either: 1) progressive, unexplained mild cognitive impairment; or 2) dementia of uncertain cause due to atypical or mixed symptoms, or unusually early age-of-onset.

Review Article

Molecular imaging in dementia: Past, present, and future

R. Laforce, Jr.[a,*], J. P. Soucy[b], L. Sellami[a], C. Dallaire-Théroux[a], F. Brunet[a], D. Bergeron[a], B. L. Miller[c], R. Ossenkoppele[d]

Alzheimer's & Dementia ■ (2018) 1-31

Specific limitations of each imaging modality and recommendations to overcome them

	Main limitations	Recommendations to overcome the limitations
Amyloid imaging	1. Expensive technique 2. Not widely available 3. Inaccurate interpretation of PET results by clinicians	1. (a) Selective use of this diagnostic tool in expert dementia centers. (b) Multiple scans can be performed using a single batch of ^{18}F-amyloid PET tracer production. 2. (a) Advent of ^{18}F-amyloid PET tracers allows distribution to hospitals without an on-site cyclotron (120 min half-life). (b) Referral can be made to proximate expert PET centers. 3. Specific guidelines (US [175] and Canada[2]) on appropriate use of amyloid imaging have been published.

$2750!

10X + than FDG, a test which is *very* good!!

Additive value of amyloid-PET in routine cases of clinical dementia work-up after FDG-PET

Eur J Nucl Med Mol Imaging (2017) 44:2239–2248

Matthias Brendel[1] · Jonas Schnabel[1] · Sonja Schönecker[2] · Leonie Wagner[1] · Eva Brendel[1] · Johanna Meyer-Wilmes[1] · Marcus Unterrainer[1] · Andreas Schildan[3] · Marianne Patt[3] · Catharina Prix[2] · Nibal Ackl[2] · Cihan Catak[4] · Oliver Pogarell[5] · Johannes Levin[2,6] · Adrian Danek[2,6] · Katharina Buerger[4,6] · Peter Bartenstein[1,7] · Henryk Barthel[3] · Osama Sabri[3] · Axel Rominger[1,7]

Abstract

Purpose In recent years, several [^{18}F]-labeled amyloid-PET tracers have been developed and have obtained clinical approval. Despite their widespread scientific use, studies in routine clinical settings are limited. We therefore investigated the impact of [^{18}F]-florbetaben (FBB)-PET on the diagnostic management of patients with suspected dementia that was still

Methods All subjects were referred in-house with a suspected dementia syndrome due to neurodegenerative disease. After undergoing an FDG-PET exam, the cases were discussed by the interdisciplinary dementia board, where the most likely diagnosis as well as potential differential diagnoses were documented. Because of persistent diagnostic uncertainty, the patients received an additional FBB-PET exam. Results were interpreted visually and classified as amyloid-positive or amyloid-negative, and we then compared the individual clinical diagnoses before and after additional FBB-PET.

Results A total of 107 patients (mean age 69.4 ± 9.7y) were included in the study. The FBB-PET was rated as amyloid-positive in 65/107. In 83% of the formerly unclear cases, a final diagnosis was reached through FBB-PET, and the most likely prior diagnosis was changed in 28% of cases. The highest impact was observed for distinguishing Alzheimer's dementia (AD) from fronto-temporal dementia (FTLD), where FBB-PET altered the most likely diagnosis in 41% of cases.

Conclusions FBB-PET has a high additive value in establishing a final diagnosis in suspected dementia cases when prior investigations such as FDG-PET are inconclusive. The differentiation between AD and FTLD was particularly facilitated by amyloid-PET, predicting a considerable impact on patient management, especially in the light of upcoming disease-modifying therapies.

Aloysius Alzheimer (Auguste D.)

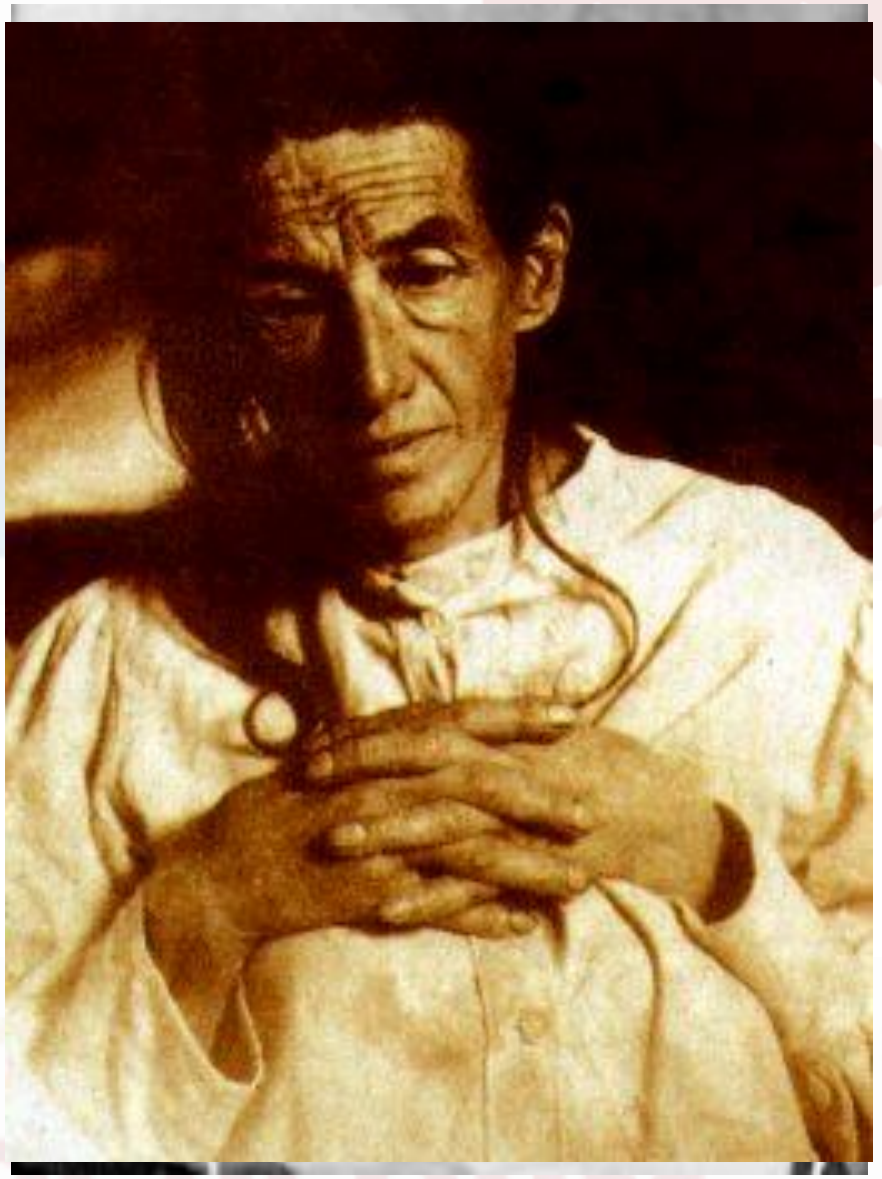

"About a strange cortical disease"

Alzheimer A (1907) Über eine eigenartige Erkrankung der Hirnrinde. Allg Zeitschr Psychiatr 64 :146–148

Plaques

NFTs

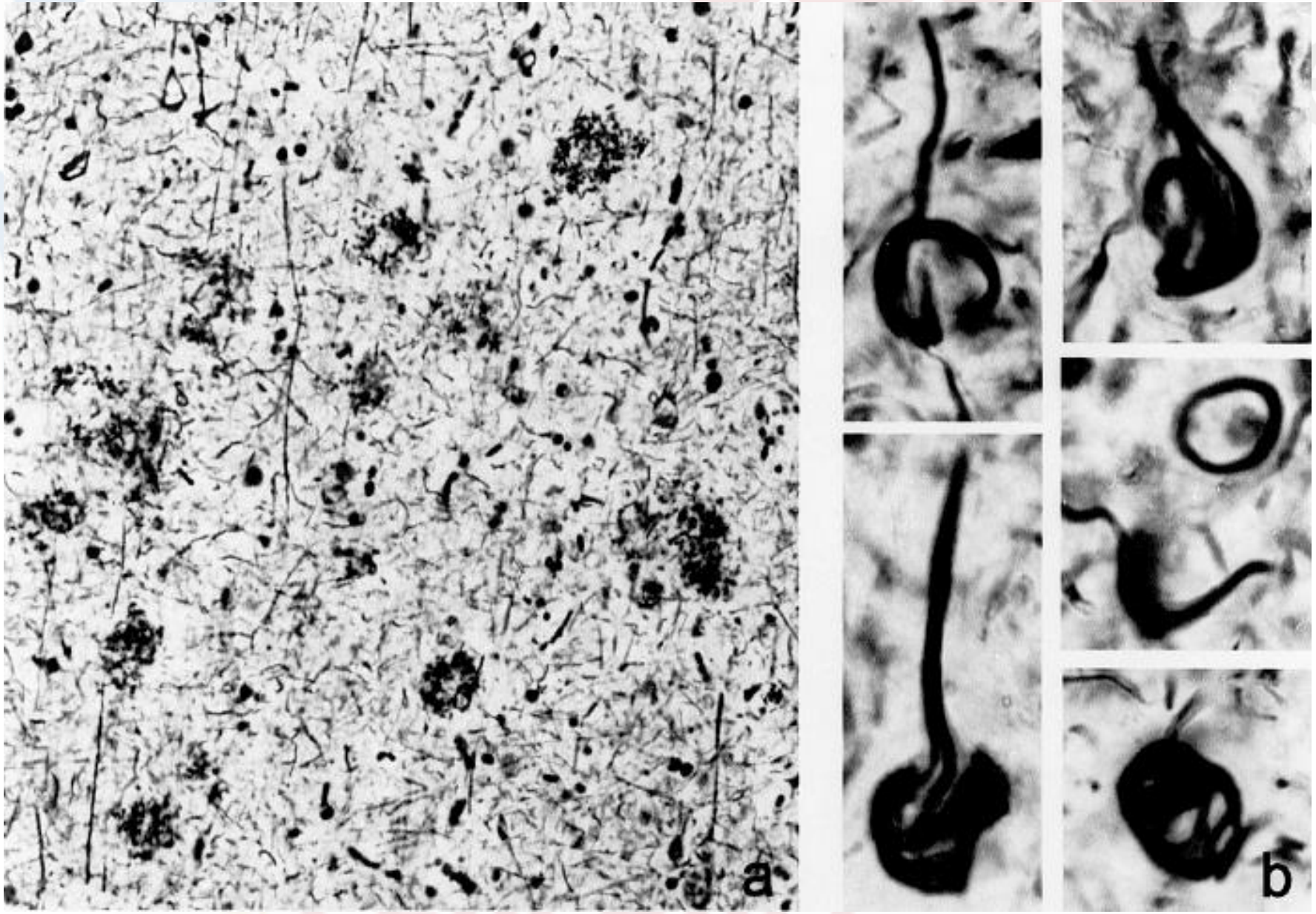

Classification of tauopathies

Tau-based therapies in neurodegeneration: opportunities and challenges

Chuanzhou Li and Jürgen Götz

NATURE REVIEWS | DRUG DISCOVERY
VOLUME 16 | DECEMBER 2017 | 863

Table 1 | **Classification of tauopathies based on cell types with prominent pathology**

Disease	Neurons	Astrocytes	Oligodendrocytes
Neuronal			
Alzheimer disease	• NFTs • Neuropil threads • Neuritic components in plaques	NA	NA
Predominantly neuronal			
Pick disease	• Pick bodies • Diffuse 'synapse-like' tau IR neuropil	(Tau-IR ramified astrocytes)	(Globular oligodendroglial inclusions)
Neuronal and glial			
Progressive supranuclear palsy	• NFTs • Neuropil threads	• Tufted astrocytes • (Diffuse granular IR)	Coiled bodies
Corticobasal degeneration	• Neuropil threads • Spherical cytoplasmic inclusions • (NFTs)	Astrocytic plaques	Coiled bodies
Argyrophilic grain disease	Argyrophilic grains	• Thorn-shaped astrocytes • Diffuse granular IR	Coiled bodies
Chronic traumatic encephalopathy	• NFTs • Neuropil threads	• Astrocytic deposits • (Tufted astrocytes) • (Thorn-shaped astrocytes)	NA
Predominantly glial			
Globular glial tauopathy	• Spherical cytoplasmic inclusions • (Neuropil threads) • (NFTs)	Globular astroglial inclusions	Globular oligodendroglial inclusions

Secondary tauopathy

Secondary tauopathies

NEVER!!!!!
AD-like

How the shapes of seeds can influence pathology

Ronald Melki

Neurobiology of Disease 109 (2018) 201–208

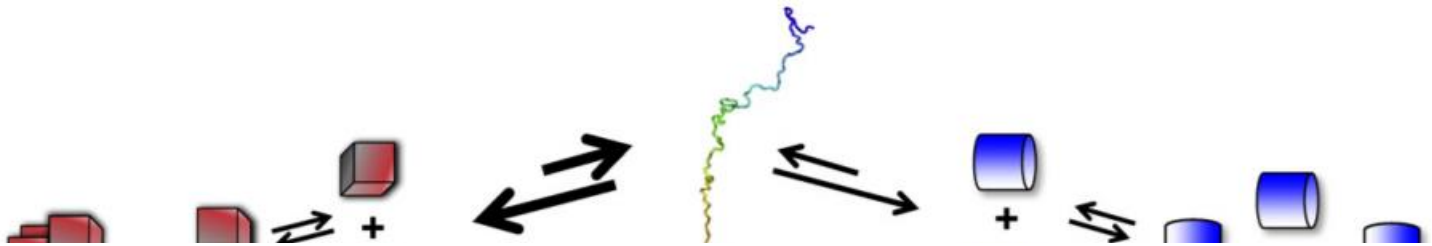

ABSTRACT

It is widely accepted that the loss of function of different cellular proteins following their aggregation into highly stable aggregates or the gain of pathologic function of the resulting macromolecular assemblies or both processes are tightly associated to distinct debilitating neurodegenerative diseases such as Alzheimer's, Parkinson's, Creutzfeldt-Jacob, Amyotrophic Lateral Sclerosis and Huntington's diseases. How the aggregation of one given protein leads to distinct diseases is unclear. Here, a structural-molecular explanation based on the ability of proteins such as α-synuclein or tau to form assemblies that differ by their intrinsic architecture, stability, seeding capacity, and surfaces is proposed to account for distinct synucleinopathies and tauopathies. The shape and surfaces of the seeds is proposed to define at the same time their seeding capacity, interactome and tropism for defined neuronal cells within the central nervous system.

Fig. 2. Schematic representation of the assembly of different protein conformers into structurally distinct, highly ordered, fibrillar polymorphs. Natively unfolded polypeptide chains (noodle shaped, rainbow colored molecule in the centre of the scheme) populate folding intermediates (red cube, blue cylinder, green diamond and yellow polyhedron) following conformational changes. The nature of the folding intermediates depends on the folding landscape of the natively unfolded polypeptide chain and its amino acid composition. The ability to populate any folding intermediate depend on its stability and life time. This is represented here by the length and thickness of the arrows. Once populated, the folding intermediates interact transiently with like conformers and establish longitudinal or lateral interactions. These interactions are reversible. They are represented here by arrows going in one direction or the other. When longitudinal and lateral interactions are established, as explained in Fig. 1, stable, highly ordered seed polymorphs are formed. The latter can grow indefinitely from both ends by incorporating the monomeric form of the conformer they are made of, yielding structurally, physically and functionally distinct fibrillar polymorphs. The arrow sizes reflect the rates that characterize the interactions between distinct folding intermediates, the stabilization of the seeds and their further growth, discussed in Fig. 1.

Imaging of Tau Pathology in a Tauopathy Mouse Model and in Alzheimer Patients Compared to Normal Controls

Neuron 79, 1094–1108, September 18, 2013

Masahiro Maruyama,[1,10] Hitoshi Shimada,[1,10] Tetsuya Suhara,[1] Hitoshi Shinotoh,[1] Bin Ji,[1] Jun Maeda,[1] Ming-Rong Zhang,[1] John Q. Trojanowski,[2] Virginia M.-Y. Lee,[2] Maiko Ono,[1] Kazuto Masamoto,[1] Harumasa Takano,[1] Naruhiko Sahara,[3,5,6] Nobuhisa Iwata,[4] Nobuyuki Okamura,[7] Shozo Furumoto,[7] Yukitsuka Kudo,[8] Qing Chang,[9] Takaomi C. Saido,[4] Akihiko Takashima,[3] Jada Lewis,[5,6] Ming-Kuei Jang,[9] Ichio Aoki,[1] Hiroshi Ito,[1] and Makoto Higuchi[1,*]

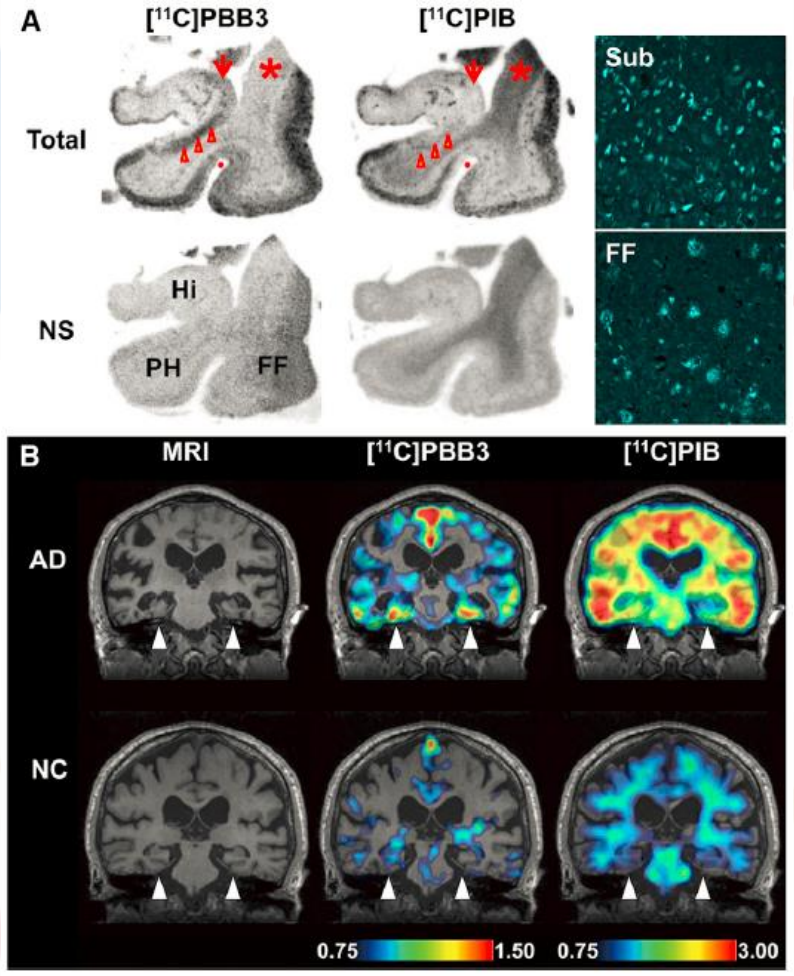

Figure 7. Accumulation of [11C]PBB3 in the Hippocampal Formation of AD Patients Revealed by In Vitro Autoradiography and In Vivo PET

Monoamine oxidase B inhibitor, selegiline, reduces ^{18}F-THK5351 uptake in the human brain

Ng et al. Alzheimer's Research & Therapy (2017) 9:25
DOI 10.1186/s13195-017-0253-y

Kok Pin Ng[1,2,3], Tharick A. Pascoal[1], Sulantha Mathotaarachchi[1], Joseph Therriault[1], Min Su Kang[1], Monica Shin[1], Marie-Christine Guiot[4], Qi Guo[5], Ryuichi Harada[6], Robert A. Comley[5], Gassan Massarweh[7], Jean-Paul Soucy[7], Nobuyuki Okamura[8], Serge Gauthier[3] and Pedro Rosa-Neto[1,3,9,10]*

Abstract

Background: ^{18}F-THK5351 is a quinoline-derived tau imaging agent with high affinity to paired helical filaments (PHF). However, high levels of ^{18}F-THK5351 retention in brain regions thought to contain negligible concentrations of PHF raise questions about the interpretation of the positron emission tomography (PET) signals, particularly given previously described interactions between quinolone derivatives and monoamine oxidase B (MAO-B). Here, we tested the effects of MAO-B inhibition on ^{18}F-THK5351 brain uptake using PET and autoradiography.

Methods: Eight participants (five mild cognitive impairment, two Alzheimer's disease, and one progressive supranuclear palsy) had baseline ^{18}F-AZD4694 and ^{18}F-THK5351 scans in order to quantify brain amyloid and PHF load, respectively. A second ^{18}F-THK5351 scan was conducted 1 week later, 1 h after a 10-mg oral dose of selegiline. Three out of eight patients also had a third ^{18}F-THK5351 scan 9–28 days after the selegiline administration. The primary outcome measure was standardized uptake value (SUV), calculated using tissue radioactivity concentration from 50 to 70 min after ^{18}F-THK5351 injection, normalizing for body weight and injected radioactivity. The SUV ratio (SUVR) was determined using the cerebellar cortex as the reference region. ^{18}F-THK5351 competition autoradiography studies in postmortem tissue were conducted using 150 and 500 nM selegiline.

Results: At baseline, ^{18}F-THK5351 SUVs were highest in the basal ganglia (0.64 ± 0.11) and thalamus (0.62 ± 0.14). In the post-selegiline scans, the regional SUVs were reduced on average by 36.7% to 51.8%, with the greatest reduction noted in the thalamus (51.8%) and basal ganglia (51.4%). MAO-B inhibition also reduced ^{18}F-THK5351 SUVs in the cerebellar cortex (41.6%). The SUVs remained reduced in the three patients imaged at 9–28 days. Tissue autoradiography confirmed the effects of MAO-B inhibition on ^{18}F-THK5351 uptake.

Conclusions: These results indicate that the interpretation of ^{18}F-THK5351 PET images, with respect to tau, is confounded by the high MAO-B availability across the entire brain. In addition, the heterogeneous MAO-B availability across the cortex may limit the interpretation of ^{18}F-THK5351 scans using reference region methods.

Keywords: ^{18}F-THK5351 tau tracer, Monoamine oxidase-B, Selegiline, Alzheimer's disease, Positron emission tomography

Off-Target ^{18}F-AV-1451 Binding in the Basal Ganglia Correlates with Age-Related Iron Accumulation

J Nucl Med 2018; 59:117–120

Jae Yong Choi[1,2], Hanna Cho[3], Sung Jun Ahn[4], Jae Hoon Lee[1], Young Hoon Ryu[1], Myung Sik Lee[3], and Chul Hyoung Lyoo[3]

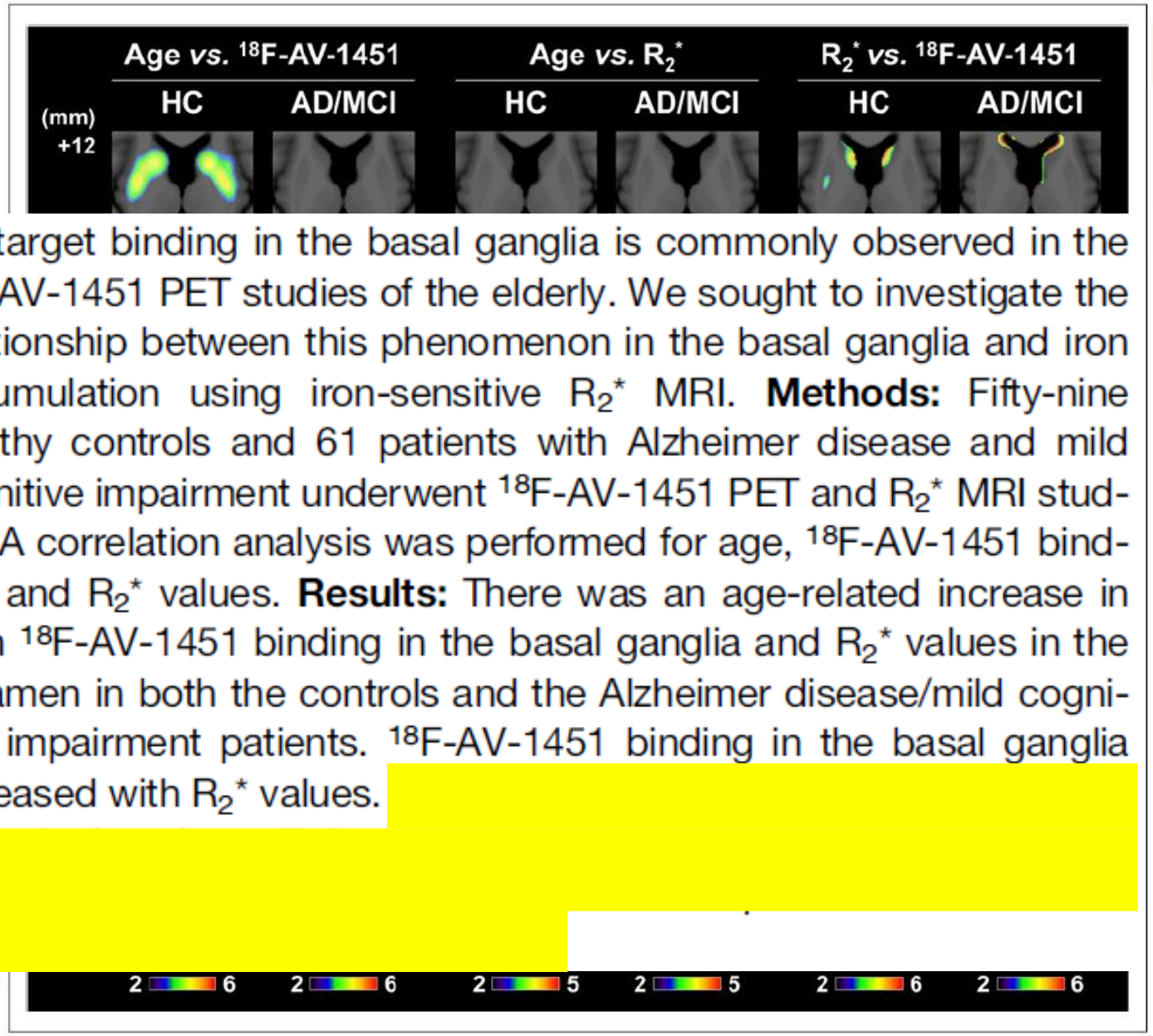

Off-target binding in the basal ganglia is commonly observed in the ^{18}F-AV-1451 PET studies of the elderly. We sought to investigate the relationship between this phenomenon in the basal ganglia and iron accumulation using iron-sensitive R_2^* MRI. **Methods:** Fifty-nine healthy controls and 61 patients with Alzheimer disease and mild cognitive impairment underwent ^{18}F-AV-1451 PET and R_2^* MRI studies. A correlation analysis was performed for age, ^{18}F-AV-1451 binding, and R_2^* values. **Results:** There was an age-related increase in both ^{18}F-AV-1451 binding in the basal ganglia and R_2^* values in the putamen in both the controls and the Alzheimer disease/mild cognitive impairment patients. ^{18}F-AV-1451 binding in the basal ganglia increased with R_2^* values.

FIGURE 2. Voxel-based analysis results for correlation among age, ^{18}F-AV-1451 SUVRs, and R_2^* values Coordinates for each slice are presented as numbers on left side of figure (distance from anterior commissure: from ventral to dorsal for axial images and from rostral to caudal for coronal images). Color scale bars represent $-\log_{10} P$ values. HC = healthy control.

Characteristics of Tau and Its Ligands in PET Imaging

Biomolecules **2016**, *6*, 7; doi:10.3390/biom6010007

Ryuichi Harada [1], Nobuyuki Okamura [1,2,*], Shozo Furumoto [3], Tetsuro Tago [3], Kazuhiko Yanai [2], Hiroyuki Arai [4] and Yukitsuka Kudo [1,3]

2. Characteristics of Tau Deposits in Neurodegenerative Conditions

2.1. Different Localization and Histopathology of Tau Deposits

2.2. Different Isoform Composition of Tau Deposits

Six isoforms of tau protein are produced by alternative splicing of the tau gene and categorized based on the number of microtubule-binding domains into two functionally different groups; three repeat (3R) or four repeat (4R) [24,25]. According to the biochemical analyses of normal adult human brain samples from fresh biopsies, six normal tau isoforms were expressed in the adult brain with approximately equal ratio of 3R and 4R tau isoforms [26]. However, abnormal tau deposits in neurodegenerative conditions contain different isoform compositions; both 3R and 4R tau in AD/TPSD/CTE: predominantly 4R tau in CBD/PSP/AGD and 3R tau in Pick's disease [20,27–29].

and layer VI in the frontal and temporal neocortex in Pick's disease [17]. Although tau deposits in CTE have similar histopathological characteristics as neurofibrillary tangles and neuropil threads, neurofibrillary tangles were observed focally in superficial cortical layers [18–20]. In PSP and CBD, tufted astrocytes, astrocytic plaques, coiled bodies, and argyrophilic threads were observed as glial tau deposits [21–23]. Tau deposits in CBD and PSP are also observed in the subcortical white matter and brainstem [22]. This evidence shows the distinct localization and histopathological characteristics of tau deposits in neurodegenerative conditions.

Tangle Predominant Senile Dementia = Limbic Variant of AD

In vivo quantification of neurofibrillary tangles with [^{18}F]MK-6240

Tharick A. Pascoal[1,2], Monica Shin[1], Min Su Kang[1,2], Mira Chamoun[2], Daniel Chartrand[2], Sulantha Mathotaarachchi[1,2], Idriss Bennacef[3], Joseph Therriault[1], Kok Pin Ng[1], Robert Hopewell[2], Reda Bouhachi[2], Hung-Hsin Hsiao[2], Andrea L. Benedet[1], Jean-Paul Soucy[2], Gassan Massarweh[2], Serge Gauthier[1] and Pedro Rosa-Neto[1,2,4*]

Pascoal *et al. Alzheimer's Research & Therapy* (2018) 10:74

Abstract

Background: Imaging agents capable of quantifying the brain's tau aggregates will allow a more precise staging of Alzheimer's disease (AD). The aim of the present study was to examine the in vitro properties as well as the in vivo kinetics, using gold standard methods, of the novel positron emission tomography (PET) tau imaging agent [^{18}F]MK-6240.

Methods: In vitro properties of [^{18}F]MK-6240 were estimated with autoradiography in postmortem brain tissues of 14 subjects (seven AD patients and seven age-matched controls). In vivo quantification of [^{18}F]MK-6240 binding was performed in 16 subjects (four AD patients, three mild cognitive impairment patients, six healthy elderly individuals, and three healthy young individuals) who underwent 180-min dynamic scans; six subjects had arterial sampling for metabolite correction. Simplified approaches for [^{18}F]MK-6240 quantification were validated using full kinetic modeling with metabolite-corrected arterial input function. All participants also underwent amyloid-PET and structural magnetic resonance imaging.

Results: In vitro [^{18}F]MK-6240 uptake was higher in AD patients than in age-matched controls in brain regions expected to contain tangles such as the hippocampus, whereas no difference was found in the cerebellar gray matter. In vivo, [^{18}F]MK-6240 displayed favorable kinetics with rapid brain delivery and washout. The cerebellar gray matter had low binding across individuals, showing potential for use as a reference region. A reversible two-tissue compartment model well described the time–activity curves across individuals and brain regions. Distribution volume ratios using the plasma input and standardized uptake value ratios (SUVRs) calculated after the binding approached equilibrium (90 min) were correlated and higher in mild cognitive impairment or AD dementia patients than in controls. Reliability analysis revealed robust SUVRs calculated from 90 to 110 min, while earlier time points provided inaccurate estimates.

Conclusions: This evaluation shows an [^{18}F]MK-6240 distribution in concordance with postmortem studies and that simplified quantitative approaches such as the SUVR offer valid estimates of neurofibrillary tangle load 90 min post injection. [^{18}F]MK-6240 is a promising tau tracer with the potential to be applied in the disease diagnosis and assessment of therapeutic interventions.

Keywords: Tau positron emission tomography, Neurofibrillary tangles, Alzheimer's disease

Appropriate tools for measuring tau levels *in vivo* are urgently needed for clinical trials!

Tau-based therapies in neurodegeneration: opportunities and challenges

Chuanzhou Li and Jürgen Götz

NATURE REVIEWS | DRUG DISCOVERY
VOLUME 16 | DECEMBER 2017 | 863

Table 2 | **Selected tau-targeted therapies in clinical development**

Name	Sponsor	Mechanism or target	Indication	Phase of clinical development	ClinicalTrials.gov identifier
TRx0237	TauRx Therapeutics	Tau aggregation	• AD • AD • AD • bvFTD • AD or bvFTD	• II (terminated) • III (completed) • III (completed) • III (completed) • III (recruiting)	• NCT01626391 • NCT01689246 • NCT01689233 • NCT01626378 • NCT02245568
ACI-35	AC Immune/ Janssen	Active vaccine, 16 copies of a tau fragment phosphorylated at S396/S404 (PHF1)	AD	Ib (completed)	(ISRCTN13033912)
AADvac-1 (REF. 112)	Axon Neuroscience SE	Active vaccine, tau 294–305	• AD • AD • AD	• I (completed) • I (completed) • II (ongoing)	• NCT01850238 • NCT02031198 • NCT02579252
RG6100 (also known as RO7105705)	Genentech	Passive vaccine, anti-tau	AD	I (completed)	NCT02820896
ABBV-8E12 (also known as C2N-8E12)	C2N/AbbVie	Passive vaccine, extracellular aggregated tau	• PSP • PSP • AD	• I (completed) • II (recruiting) • II (recruiting)	• NCT02494024 • NCT02985879 • NCT02880956
BMS-986168*	BMS/iPierian	Passive vaccine, N-terminally truncated tau	• Tauopathies (healthy individuals)	• I (completed)	• NCT02294851
			• PSP • PSP	• I (completed) • II (recruiting)	• NCT02460094 • NCT03068468
IVIG	• Sutter Health • Baxalta US	Pooled immunoglobulin	• MCI • AD • AD • AD	• II (ongoing) • III (terminated) • III (terminated) • III (completed)	• NCT01300728 • NCT01524887 • NCT01736579 • NCT00818662
	• WMCCU • Octapharma • Instituto Grifols		• AD • AD • AD	• II (completed) • II (completed) • II/III (ongoing)	• NCT00299988 • NCT00812565 • NCT01561053
Davunetide (NAP; AL-108)	• Allon Therapeutics • UCSF	Neuroprotective via microtubule stabilization	• MCI • MCI • PSP • Predicted tauopathies	• II (completed) • II (completed) • II/III (completed) • II (ongoing)	• NCT00422981 • NCT00404014 • NCT01110720 • NCT01056965
TPI-287	UCSF	Microtubule stabilizer	• AD • PSP or CBS	• I (ongoing) • I (ongoing)	• NCT01966666 • NCT02133846
ANAVEX 2-73	Anavex	σ_1/muscarinic ligand	• AD • AD	• IIa (ongoing) • II (recruiting)	• NCT02244541 • NCT02756858
MK-8719	Alectos	OGA inhibitor	PSP	I (granted orphan drug designation for PSP)	Not available
AZD0530 (also known as saracatinib)	Yale University/ AstraZeneca	Fyn	• AD • AD	• I (completed) • II (ongoing)	• NCT01864655 • NCT02167256

AD, Alzheimer disease; bvFTD, behavioural variant of frontotemporal dementia; CBS, corticobasal syndrome; MCI, mild cognitive impairment; OGA, O-GlcNAcase; PSP, progressive supranuclear palsy. *Discovered using induced pluripotent stem cells from patients with AD[227].

Plan/Objectives

- The established:
  ^{18}F-FDG: old, but still going strong!/ A quick, brief, not long, short discussion to remember that it's still the best we have

- The almost there:
  - Amyloid PET Imaging: good, work-in-progress/ Understand what it means to find plaques in the brain in order to define clinical indications
  - Tau imaging/ Recognize that it's great for research, and might also be for patients

- The future / Review some avenues that will keep us relevant

Hey! Everybody does it! Must have some usefulness …

Use of [redacted] imaging and [redacted] for diagnosis and prognosis of early stages of Alzheimer's disease

Translational Research 2018;194:56–67

XIAONAN LIU, KEWEI CHEN, TERESA WU, DAVID WEIDMAN, FLEMING LURE, and JING LI

Table III. Summary of studies using multimodality imaging for AD prognosis at early stage

Articles	Stage	Imaging modalities	Nonimaging data	Cross-sectional or longitudinal	ML model	Data source	Sample size	Acc.	Sens.	Spec.
Ritter et al.[16]	MCI	MRI, FDG-PET	CSF, neuropsychological testing, medical history, symptoms, neurologic and physical examinations, and demographics	Cross-sectional	SVM	ADNI	86 MCI-c vs 151 MCI-nc	0.730	0.405	0.913
Shaffer et al.[17]	MCI	MRI, FDG-PET	CSF, neuropsychological testing, APOE, age, and education	Cross-sectional	ICA and logistic regression	ADNI	43 MCI-c vs 54 MCI-nc	0.716	0.853	0.862
Zhang et al.[18]	MCI	MRI, FDG-PET	CSF	Cross-sectional	MKL	ADNI	51 ADs, 43 MCI-c, 56 MCI-nc, 52 NCs	0.764	0.818	0.660
Liu et al.[19]	MCI	MRI, FDG-PET	None	Cross-sectional	LASSO and MKL	ADNI	44 MCI-c vs 56 MCI-nc	0.678	0.649	0.700
Zhang and Shen[20]	MCI	MRI, FDG-PET	CSF	Cross-sectional	Multitask learning and SVM	ADNI	40 ADs, 38 MCI-c, 42 MCI-nc, 47 NCs	0.739	0.686	0.736
Cheng et al.[21]	MCI	MRI, FDG-PET	CSF	Cross-sectional	Transfer learning and group LASSO	ADNI	51 ADs, 43 MCI-c, 56 MCI-nc, 52 NCs	0.794	0.845	0.727
Young et al.[22]	MCI	MRI, FDG-PET	CSF and APOE	Cross-sectional	GP for AD vs NC, applied to MCI	ADNI	47 MCI-c vs 96 MCI-nc	0.741	0.787	0.656
Hinrichs et al.[23]	MCI	MRI, FDG-PET	CSF, APOE, and NeuroPshychological Status Exam scores	Longitudinal	MKL for AD vs NC, applied to MCI	ADNI	48 ADs, 119 MCIs, 66NCs	0.791	N/A	N/A
Zhang and Shen[24]	MCI	MRI, FDG-PET	CSF, MMSE, and ADAS-Cog	Longitudinal	MKL	ADNI	35 MCI-c vs 50 MCI-nc	0.784	0.79	0.780
Wang et al.[25]	MCI	MRI, FDG-PET, florbetapir-PET	ADAS-Cog	Cross-sectional	PLS	ADNI	64 MCI-c vs 65 MCI-nc	0.861	0.813	0.907

A [redacted] to Predict a Diagnosis of Alzheimer Disease by Using ^{18}F-FDG PET of the Brain

Radiology 2018; 00:1–9 • https://doi.org/10.1148/radiol.2018180958

Yiming Ding • Jae Ho Sohn, MD, MS • Michael G. Kawczynski, MS • Hari Trivedi, MD • Roy Harnish, MS • Nathaniel W. Jenkins, MS • Dmytro Lituiev, PhD • Timothy P. Copeland, MPP • Mariam S. Aboian, MD, PhD • Carina Mari Aparici, MD • Spencer C. Behr, MD • Robert R. Flavell, MD, PhD • Shih-Ying Huang, PhD • Kelly A. Zalocusky, PhD • Lorenzo Nardo, PhD • Youngho Seo, PhD • Randall A. Hawkins, MD, PhD • Miguel Hernandez Pampaloni, MD, PhD • Dexter Hadley, MD, PhD • Benjamin L. Franc, MD, MS

Table 2: Performance Comparison of Deep Learning Algorithm and Radiology Readers

Parameter	Sensitivity (%)*	Specificity (%)*	Precision (%)*	F1 Score (%)	No. of Imaging Studies
Deep learning model on 10% ADNI set					
AD	81 (29/36)	94 (143/152)	76 (29/38)	78	36
MCI	54 (43/79)	68 (74/109)	55 (43/78)	55	79
Non-AD/MCI	59 (43/73)	75 (86/115)	60 (43/72)	59	73
Deep learning model on independent test set					
AD	100 (7/7)†	82 (27/33)	54 (7/13)	70†	7
MCI	43 (3/7)†	58 (19/33)	18 (3/17)†	25†	7
Non-AD/MCI	35 (9/26)	93 (13/14)†	90 (9/10)†	50	26
Radiology readers on independent test set					
AD	57 (4/7)	91 (30/33)	57 (4/7)	57	7
MCI	14 (1/7)	76 (25/33)	11 (1/9)	13	7
Non-AD/MCI	77 (20/26)	71 (10/14)	83 (20/24)	80	26

Note.–Unless otherwise indicated, data are averages ± standard deviation. ADNI = Alzheimer's Disease Neuroimaging Initiative, AD = Alzheimer disease, MCI = mild cognitive impairment, Non-AD/MCI = neither Alzheimer disease nor mild cognitive impairment.

* Numbers in parentheses are raw data used to calculate the percentage.

† Numbers indicate higher performance from deep learning algorithm compared with reader performance on independent test set.

P154: Random forests of amyloid PET may pinpoint key brain regions predictive of MoCA score

Katherine Zukotynski[14], Vincent Gaudet[2], Phillip Kuo[3], Sabrina Adamo[4], Maged Goubran[4], Christopher Scott[4], Christian Bocti[5], Michael Borrie[6], Howard Chertkow[7], Richard Frayne[8], Robin Hsiung[9], Robert Jr. Laforce[10], Michael Noseworthy[1], Frank Prato[6], Jim Sahlas[1], Eric Smith[11], Vesna Sossi[9], Alex Thiel[7], Jean-Paul Soucy[12], Jean-Claude Tardif[13], Sandra Black[4]

Objectives: To evaluate if random forests (RF) using amyloid PET quantitative data can identify brain regions correlating with Montreal Cognitive Assessment (MoCA) scores.

Methods: Fifty-five participants with mild cognitive impairment (MCI), early Alzheimer's disease (AD) or transient ischemic events (Mini Mental Status Examination score>20) and severe periventricular hyperintensities (Fazekas score=3) were recruited from memory (37) and stroke (18) clinics. Each participant had an (18)F-florbetapir PET (clinical read: 22 positive, 33 negative for amyloid deposition) processed using a MINC toolkit with SUVRs calculated for 59 regions of interest (ROIs) normalized to cerebellar grey matter. MoCA scores for each participant were categorized as: normal (≥26; 18 cases) or impaired (<26; 37 cases). SUVRs (not clinical reads) and MoCA categories were used to train an RF classifier with the objective of determining key ROIs for predicting MoCA score.

Results: A 100,000-tree RF (12 cases and 12 features per tree) was trained with 55 cases. The most frequent root node feature (number of trees, mean SUVR for decision, standard deviation) was: 1) right posterior cingulate (5147, 1.35, 0.19), 2) right precuneus (3901, 1.19, 0.15), 3) left posterior cingulate (3792, 1.27, 0.21), 4) left precuneus (3577, 1.21, 0.20), and 5) right anterior cingulate gyrus (3208, 1.24, 0.18). A 100,000-tree RF (10 cases, 12 features per tree) was constructed using 37 cases from memory clinics (8 normal, 29 impaired). The most frequent root node feature was: 1) right posterior cingulate (5022, 1.36, 0.16), 2) left posterior cingulate (4690, 1.26, 0.20), 3) left precuneus (4345, 1.07, 0.12), 4) left middle orbitofrontal gyrus (3748, 1.27, 0.14), and 5) right middle orbitofrontal gyrus (3745, 1.30, 0.13).

Conclusions: RFs using amyloid PET quantitation may identify key brain regions predictive of MoCA score. More data is needed to demonstrate classification accuracy.

Neuroscience 2015

Program# 828.03

Development of a PET tracer that targets amyloid β oligomers (AβOs)

*K. L. VIOLA[1], T.-T. CHANG[3,4], E. N. CLINE[1], E. CHUNG[5], M. DYKSTRA[3,4], B. MERRIFIELD[3,4], A. PECK[3,4], A. L. QIN[1], C. VALDEZ[1], H. J. WEISS[1], L. R. ZIESKE[6], W. L. KLEIN[1,2];

We will need new tracers!!

Remember:
Plaques are what we can see, but NOT the toxic form of amyloid:
Aβ oligomers are!

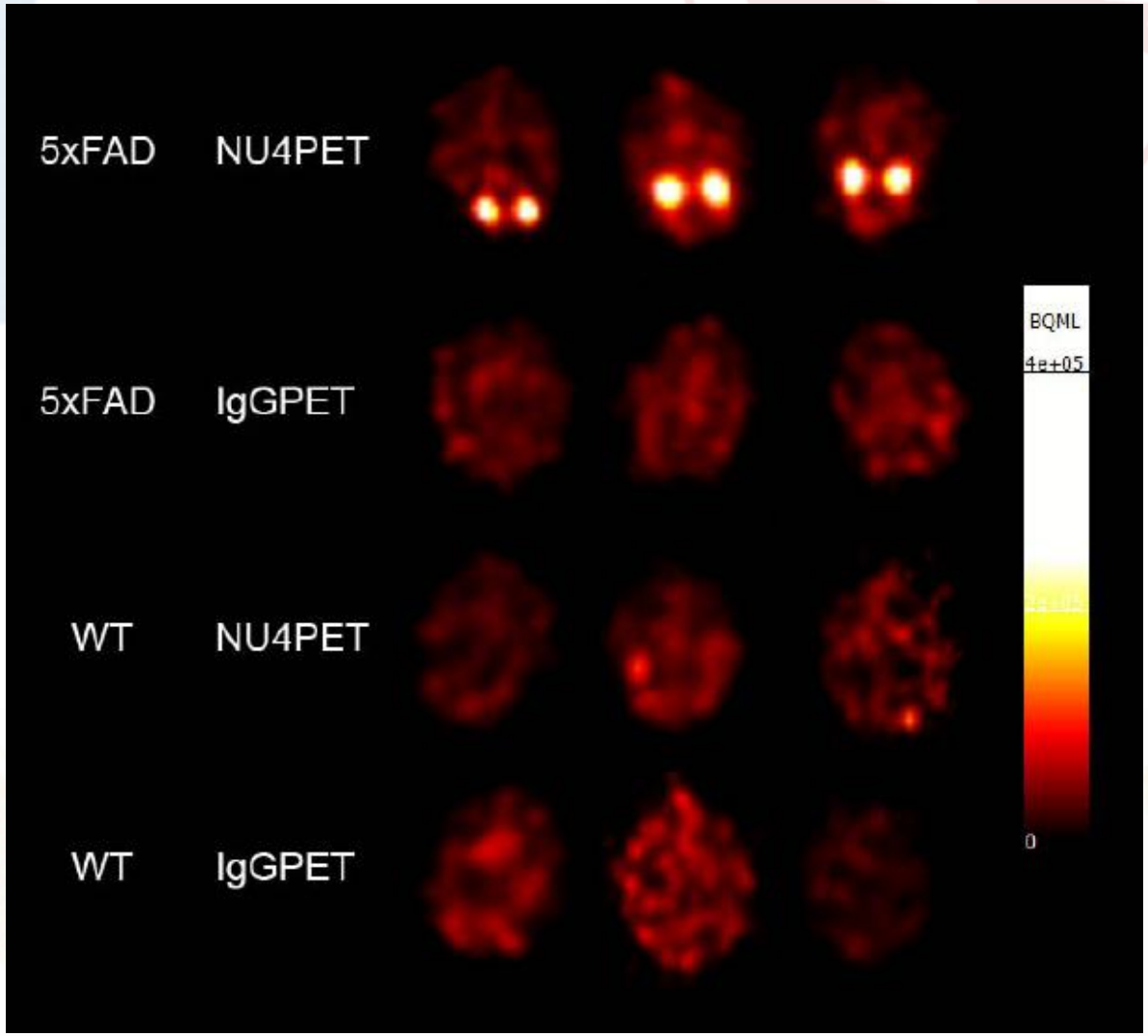

IMMEDIATE COMMUNICATION

Molecular Psychiatry advance online publication, 12 September 2017; doi:10.1038/mp.2017.183

Quantification of brain cholinergic denervation in Alzheimer's disease using PET imaging with [^{18}F]-FEOBV

M Aghourian[1,2,3], C Legault-Denis[1,2,3], J-P Soucy[2,4,5], P Rosa-Neto[2,3,4], S Gauthier[3,4], A Kostikov[2,4], P Gravel[2] and M-A Bedard[1,2,3]

^{18}FDG is very good, but there might be better.

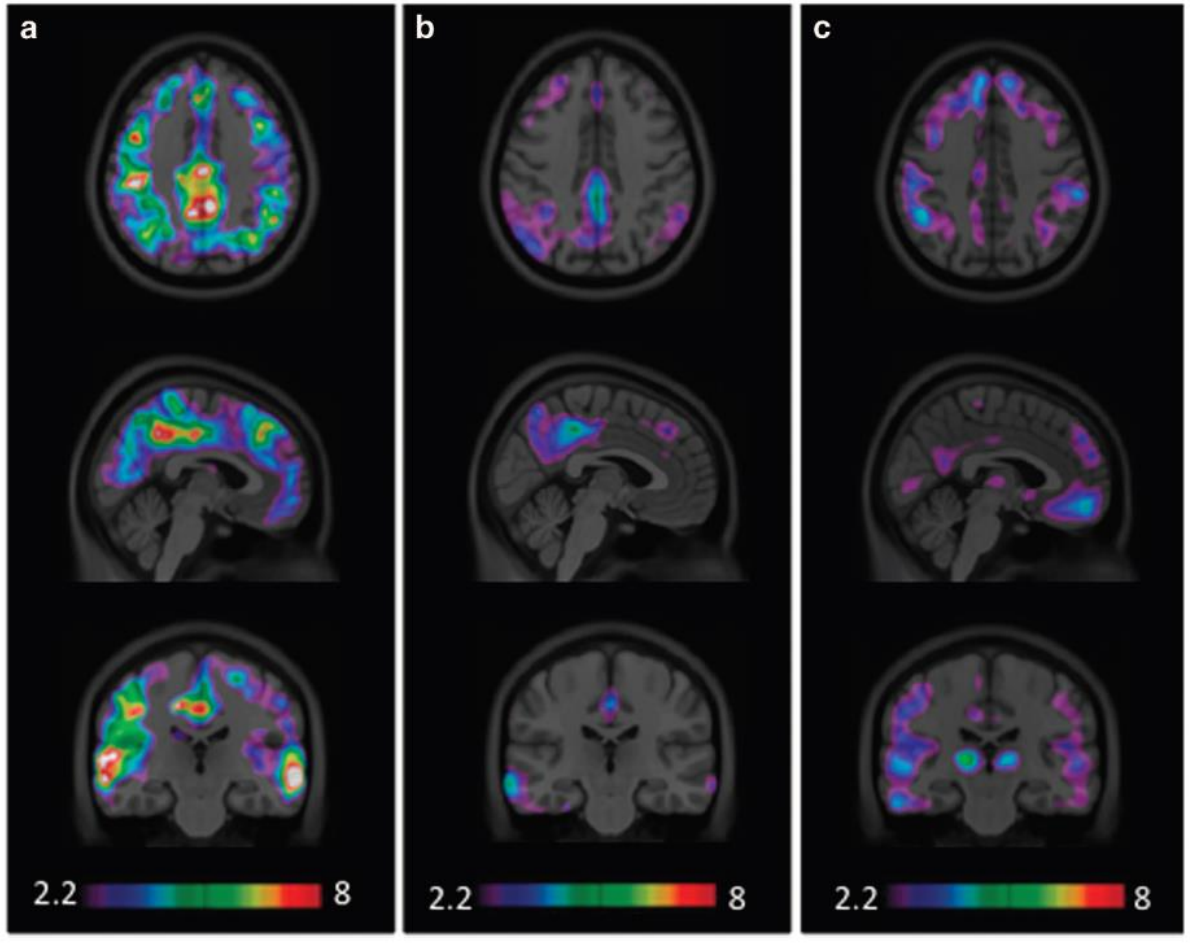

Figure 3. Brain mapping showing the voxel based significant differences (*t* values) between healthy controls, and patients with AD for FEOBV (**a**), FDG (**b**) and NAV (**c**). Although all radiotracers revealed abnormalities in similar cortical areas, more extended territories and greater intergroup differences were detected with FEOBV than with the two other radiotracers. Scales are the same for the three tracers allowing comparisons. AD, Alzheimer's disease; FDG, ^{18}F-Fluorodeoxyglucose; FEOBV, 18F-fluoroethoxybenzovesamicol; NAV, ^{18}F-NAV4694.

A Kinome-Wide Selective Radiolabeled TrkB/C Inhibitor for in Vitro and in Vivo Neuroimaging: Synthesis, Preclinical Evaluation, and First-in-Human

DOI: 10.1021/acs.jmedchem.7b00396
J. Med. Chem. 2017, 60, 6897−6910

Vadim Bernard-Gauthier,[*,†,▲,ID] Justin J. Bailey,[†] Andrew V. Mossine,[‡] Simon Lindner,[§] Lena Vomacka,[§] Arturo Aliaga,[∥] Xia Shao,[‡] Carole A. Quesada,[‡] Phillip Sherman,[‡] Anne Mahringer,[⊥] Alexey Kostikov,[#] Marilyn Grand'Maison,[▽] Pedro Rosa-Neto,[∥] Jean-Paul Soucy,[○] Alexander Thiel,[#,◆] David R. Kaplan,[¶,+] Gert Fricker,[⊥] Björn Wängler,[□] Peter Bartenstein,[§] Ralf Schirrmacher,[*,†,∞] and Peter J. H. Scott[‡,●,∞]

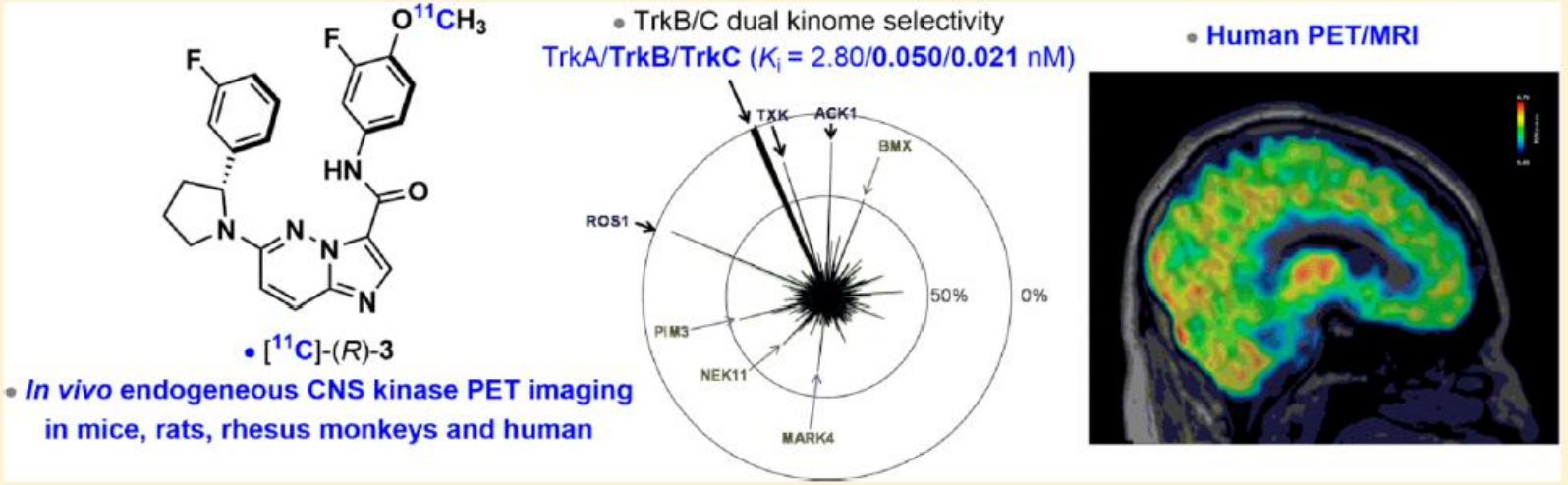

ABSTRACT: The proto-oncogenes *NTRK1/2/3* encode the tropomyosin receptor kinases TrkA/B/C which play pivotal roles in neurobiology and cancer. We describe herein the discovery of [^{11}C]-(*R*)-**3** ([^{11}C]-(*R*)-IPMICF16), a first-in-class positron emission tomography (PET) TrkB/C-targeting radiolabeled kinase inhibitor lead. Relying on extensive human kinome vetting, we show that (*R*)-**3** is the most potent and most selective TrkB/C inhibitor characterized to date. It is demonstrated that [^{11}C]-(*R*)-**3** readily crosses the blood−brain barrier (BBB) in rodents and selectively binds to TrkB/C receptors in vivo, as evidenced by entrectinib blocking studies. Substantial TrkB/C-specific binding in human brain tissue is observed in vitro, with specific reduction in the hippocampus of Alzheimer's disease (AD) versus healthy brains. We additionally provide preliminary translational data regarding the brain disposition of [^{11}C]-(*R*)-**3** in primates including first-in-human assessment. These results illustrate for the first time the use of a kinome-wide selective radioactive chemical probe for endogenous kinase PET neuroimaging in human.

Review

Radioligands for Tropomyosin Receptor Kinase (Trk) Positron Emission Tomography Imaging

Ralf Schirrmacher [1,*], Justin J. Bailey [1], Andrew V. Mossine [2], Peter J. H. Scott [2,3], Lena Kaiser [4], Peter Bartenstein [4], Simon Lindner [4], David R. Kaplan [5], Alexey Kostikov [6], Gert Fricker [7], Anne Mahringer [7], Pedro Rosa-Neto [8], Esther Schirrmacher [1], Carmen Wängler [9], Björn Wängler [10], Alexander Thiel [6,11], Jean-Paul Soucy [6] and Vadim Bernard-Gauthier [12,13,*]

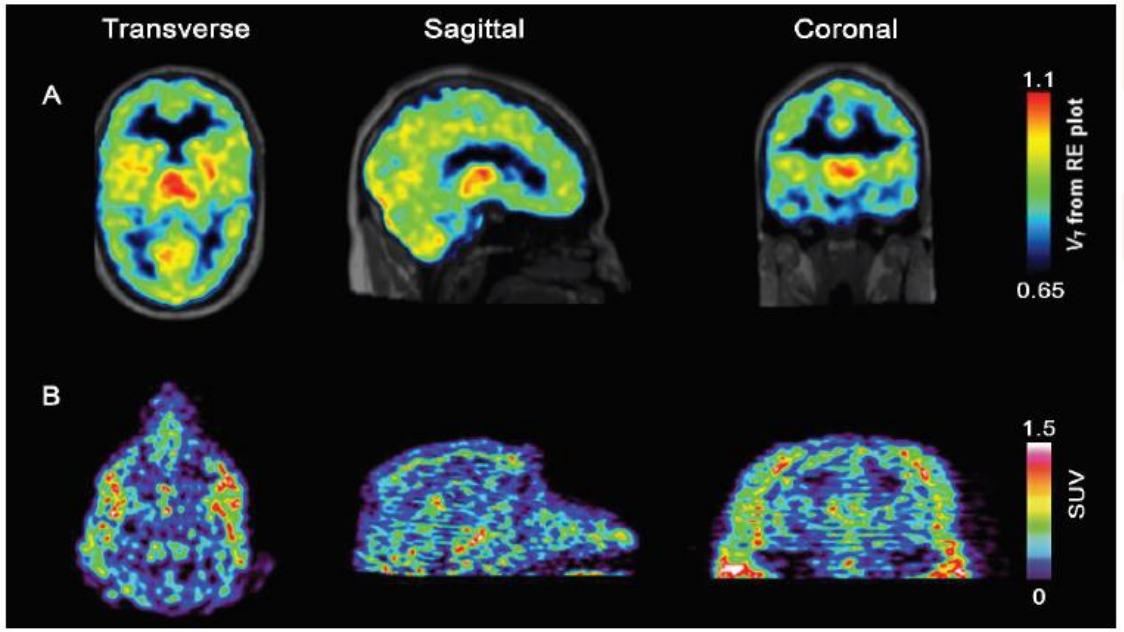

Figure 7. Upper row: PET/T1MP-RAGE MRT in vivo overlay images of [^{11}C]-(R)-12 in a human subject with high SUVs in TrkB/C rich compartments such as thalamus, followed by cerebellum and cortical grey matter and low uptake in Trk devoid white matter areas; Bottom row: In vivo PET images of [^{18}F]-(*R*)-13 (high A_m of 245 GBq/μmol) in rhesus monkey brain matching the expected TrkB/C distribution.

Abstract: survival, and differentiation during development, adult life, and aging. TrkA/B/C downregulation is a prominent hallmark of various neurological disorders including Alzheimer's disease (AD). Abnormally expressed or overexpressed full-length or oncogenic fusion TrkA/B/C proteins were shown to drive tumorigenesis in a variety of neurogenic and non-neurogenic human cancers and are currently the focus of intensive clinical research. Neurologic and oncologic studies of the spatiotemporal alterations in TrkA/B/C expression and density and the determination of target engagement of emerging antineoplastic clinical inhibitors in normal and diseased tissue are crucially needed but have remained largely unexplored due to the lack of suitable non-invasive probes. Here, we review the recent development of carbon-11- and fluorine-18-labeled positron emission tomography (PET) radioligands based on specifically designed small molecule kinase catalytic domain-binding inhibitors of TrkA/B/C. Basic developments in medicinal chemistry, radiolabeling and translational PET imaging in multiple species including humans are highlighted.

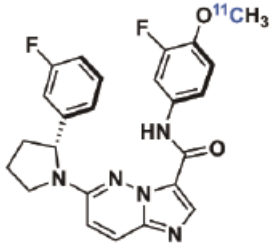

[^{11}C]-(*R*)-IPMICF16
([^{11}C]-(*R*)-**12**)

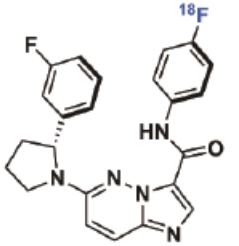

[^{18}F]TRACK
([^{18}F]-(*R*)-**13**)

Table 1 | **Attractive immune targets for manipulating AD pathology at various levels of validation**

Immune target or signalling pathway	Function	Therapeutic manipulation	Refs
TREM2 or TYROBP	Promotes Aβ uptake and/or sustains microglia or myeloid cell response to Aβ through sensing	Unclear whether targets should be upregulated or inhibited (to date, the collected *in vivo* data	20–22,89–92

Immune attack: the role of inflammation in Alzheimer disease

Frank L. Heppner[1,2], Richard M. Ransohoff[3] and Burkhard Becher[4]

Abstract | The past two decades of research into the pathogenesis of Alzheimer disease (AD) have been driven largely by the amyloid hypothesis; the neuroinflammation that is associated with AD has been assumed to be merely a response to pathophysiological events. However, . These insights have suggested both novel and well-defined potential therapeutic targets for AD, including microglia and several cytokines. In addition, as inflammation in AD primarily concerns the innate immune system — unlike in 'typical' neuroinflammatory diseases such as multiple sclerosis and encephalitides — the concept of neuroinflammation in AD may need refinement.

	member of the transforming growth factor-β family of cytokines	Unclear (overproduction reduces Aβ burden; inhibition in myeloid cells reduces Aβ burden)	167–170

Aβ, amyloid-β; AD, Alzheimer disease; APOE, apolipoprotein E; CR1, complement receptor 1; CX3CR1, CX3C chemokine receptor 1; DAMPs, damage-associated molecular patterns; IL, interleukin; MD2, NLRP3, NACHT, LRR and PYD domains-containing protein 3; PPARγ, peroxisome proliferator-activated receptor-γ; RXR, retinoic acid receptor RXR; SCARA1, macrophage scavenger receptor types I and II; TGFβ1, transforming growth factor β1; TLR4, Toll-like receptor 4; TNF, tumour necrosis factor; TNFR, TNF receptor; TREM2, triggering receptor expressed on myeloid cells 2; TYROBP, TYRO protein tyrosine kinase-binding protein.

Imaging neuroinflammation in Alzheimer's disease and other dementias:

Ne *UK*

tia 11 (2015) 1110-1120

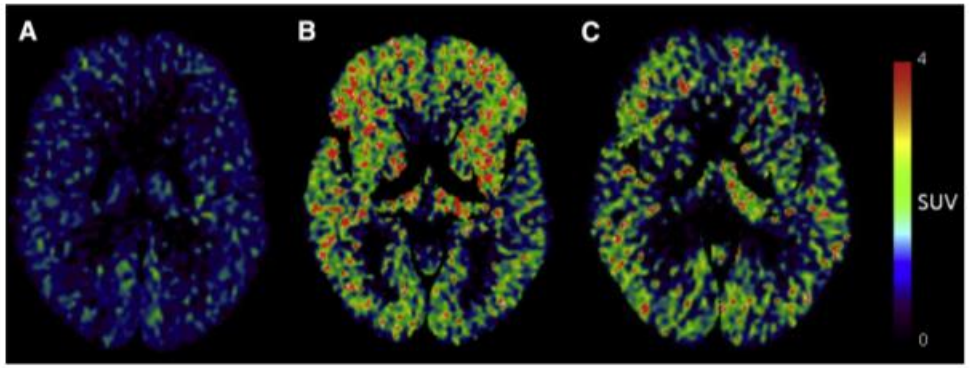

Fig. 1. [^{11}C]PK11195 BP in healthy control, AD and PDD subjects. Fig. 1 compares microglial activation in [^{11}C]PK11195 in healthy controls (A) to patients with AD (B) and patients with PDD (C), where significant activation is seen.

Abstract

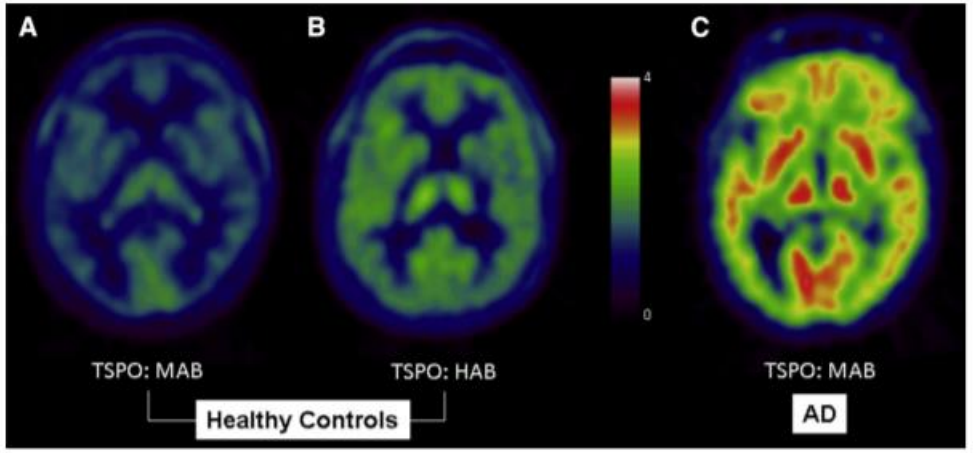

Fig. 2. [^{11}C]PBR28 BP in healthy controls compared with AD subjects. Fig. 2 compares microglial activation as quantified by the second generation TSPO ligand [^{11}C]PBR28 in (A) healthy control medium affinity binders (MABs), (B) healthy control high affinity binders (HABs) and (C) AD MAB patients.

Keywords:
TSPO; MRI

But there is more than AD!

Novel PET Tracers of α-Synuclein for the Diagnosis of Parkinson's Disease

AC Immune

Biogen

Target engagement on early PD Braak stage III-IV

Representative results of staining amygdala tissue sections

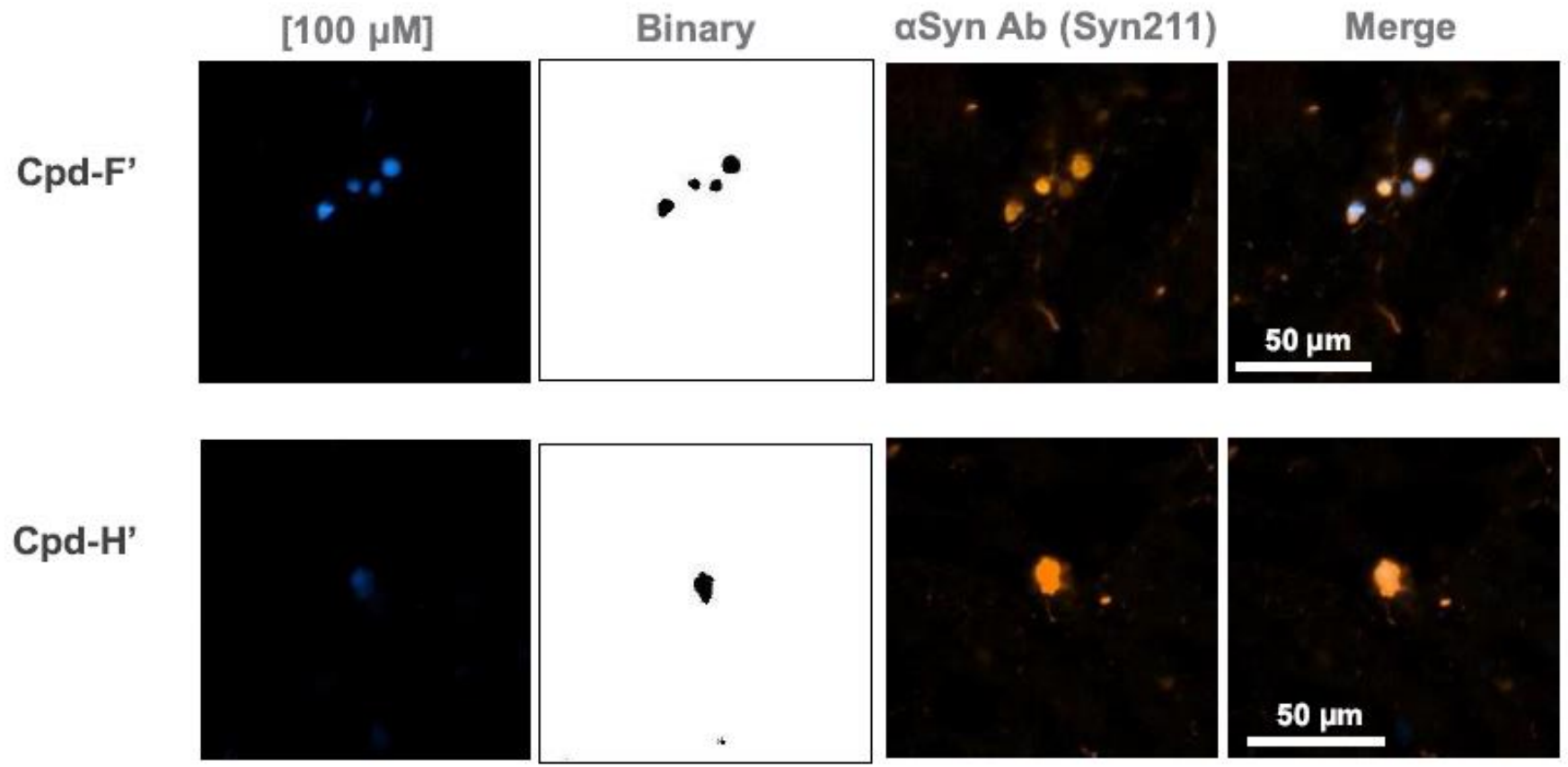

And we
want them all!!!

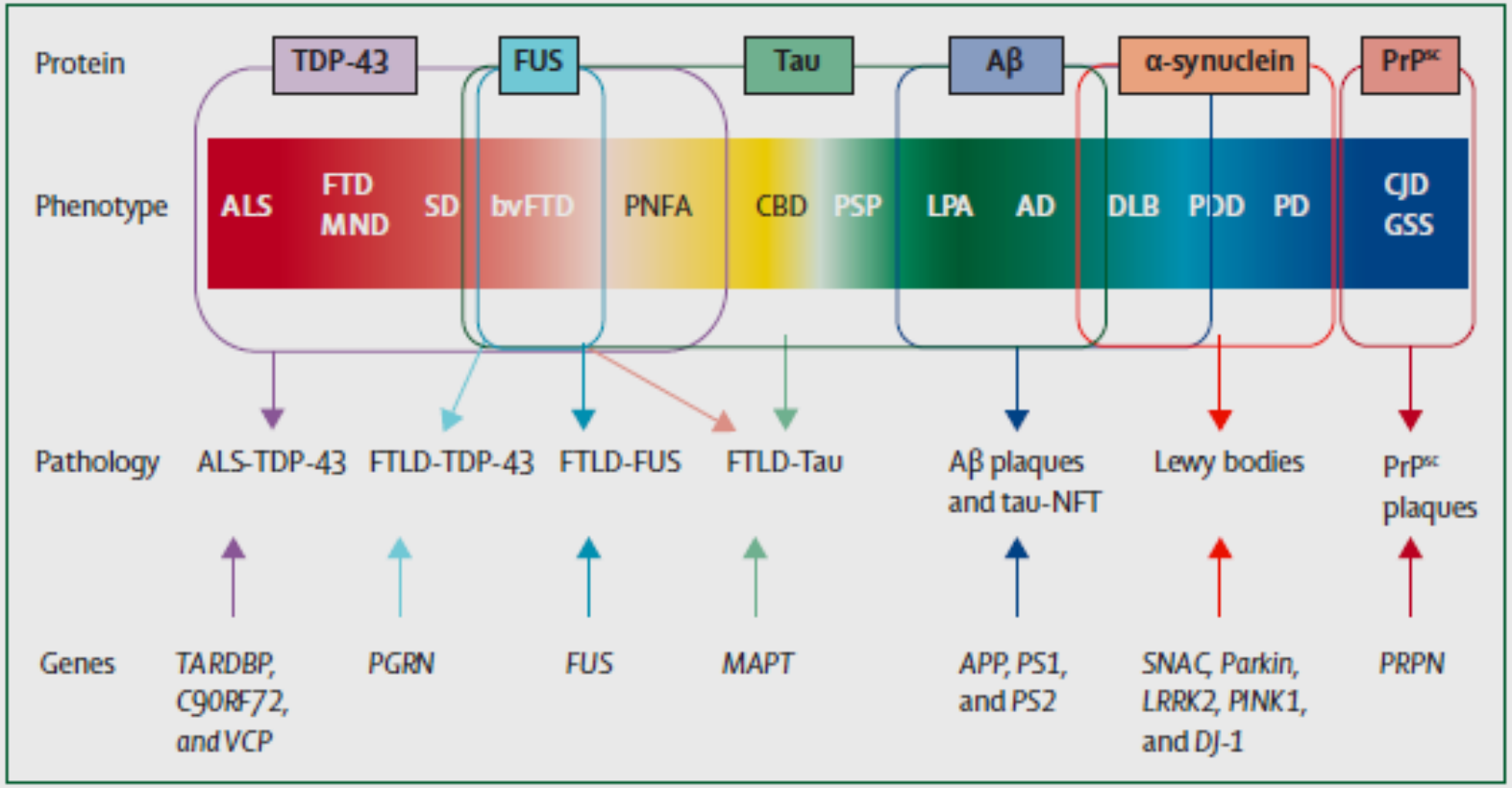

Figure 1: **Clinical, genetic, and pathological spectrum of misfolded proteins in neurodegenerative disease**
Several neurodegenerative diseases are associated with a misfolded and aggregated protein, such that the same misfolded protein is found in different clinical phenotypes and the same phenotype might be the result of different misfolded proteins. Adapted from Chen-Plotkin and colleagues,[16] by permission of Macmillan Publishers; from Rabinovici and colleagues,[17] by permission of Springer Science and Business Media; and from Seelaar and colleagues,[18] by permission of BMJ publishing group. ALS=amyotrophic lateral sclerosis. FTD MND=frontotemporal dementia with motor neuron disease. SD=semantic dementia. bvFTD=behavioural frontotemporal dementia. PNFA=progressive non-fluent aphasia. CBD=corticobasal degeneration. PSP=progressive supranuclear palsy. LPA=logopenic aphasia. AD=Alzheimer's disease. DLB=dementia with Lewy bodies. PDD=Parkinson's disease dementia. PD=Parkinson's disease. CJD=Creutzfeldt-Jakob disease. GSS=Gerstmann-Sträussler-Scheinker disease. NFT=neurofibrillary tangle.

Victor L Villemagne, Michelle T Fodero-Tavoletti, Colin L Masters, Christopher C Rowe

Lancet Neurol **2015; 14: 114–24**

Accepted 12/2018
Sleep

Brain Cholinergic Alterations in REM Sleep Behaviour Disorder: A PET Imaging Study with ^{18}F-FEOBV

Marc-Andre Bedard, PhD [1,2], Meghmik Aghourian, MSc [1,2], Camille Legault-Denis, MSc [1,2], Ronald B Postuma MD, MSc [3,4], Jean-Paul Soucy, MD, MSc [2,5,6], Jean-François Gagnon, PhD [1,3], Amélie Pelletier, PhD [3], Jacques Montplaisir, MD, PhD [3,7]

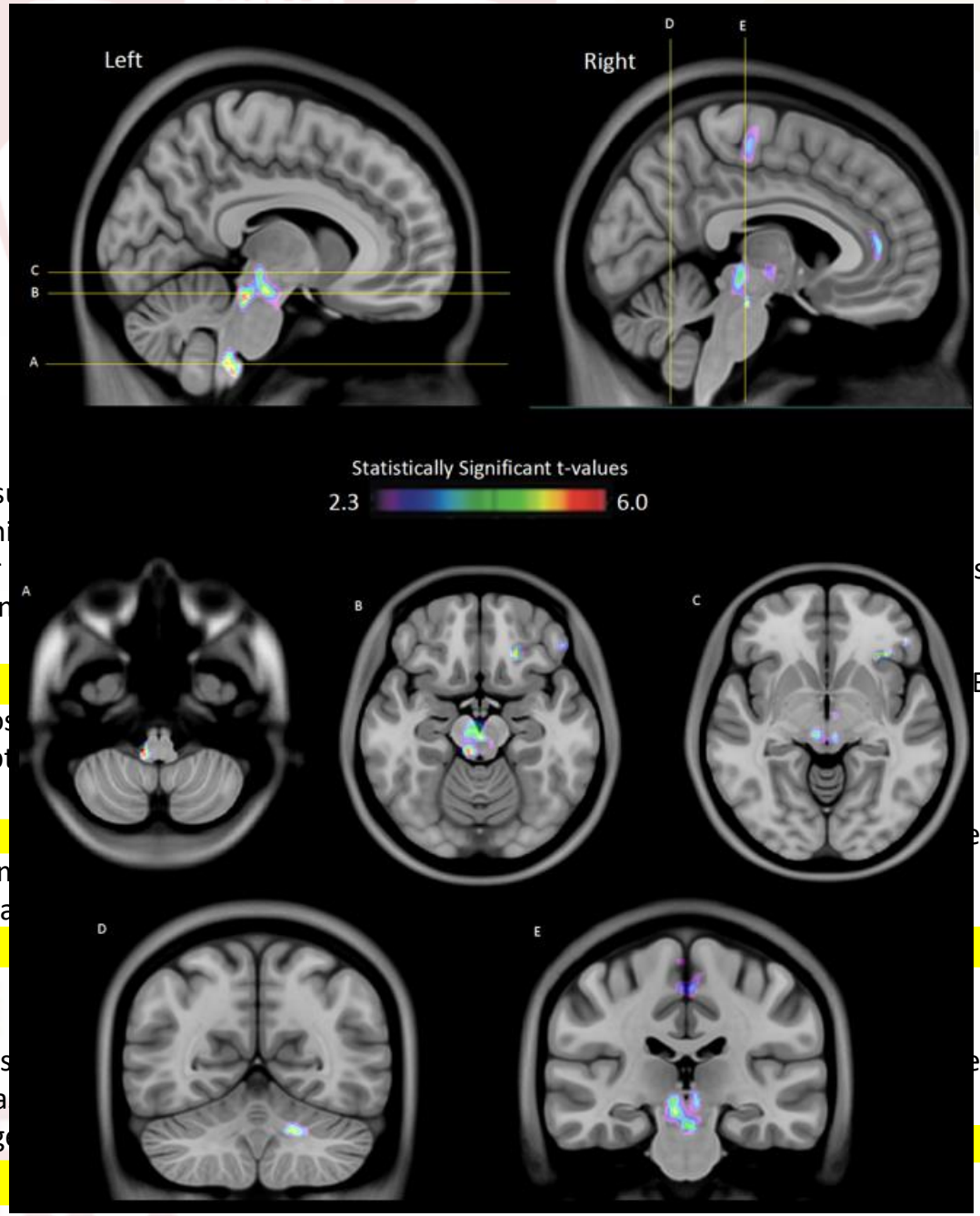

Background:
REM sleep behaviour disorder (RBD) occurs frequently in patients with synucleinopathies s
atrophy, but may also occur as a prodromal stage of those diseases, and is termed idiopath
degeneration of the mesopontine nuclei have been described in synucleinopathies with or
cholinergic neuronal integrity in iRBD using PET neuroimaging with the ^{18}F-fluoroethoxyben
Methods:
The sample included
PET imaging with FEOBV was performed in all participants. Standardized uptake value ratios
Non-parametric correlations were also computed in patients with iRBD between FEOBV up
Results:
Compared with healthy participants,
areas corresponding to the bulbar reticular formation, pontine coeruleus/subcoeruleus co
FEOBV uptake in iRBD was also higher than in controls in the ventromedial area of the thala
paracentral lobule, anterior cingulate, and orbitofrontal cortex.
Conclusion:
We showed here for the first time the brain cholinergic alterations in patients with iRBD. As
with clinical Parkinson's disease, increased cholinergic innervation is found in multiple area
containing structures involved in the promotion of REM sleep and muscle atonia. This sugg

Other "targetable" systems

Glutamatergic Transmission

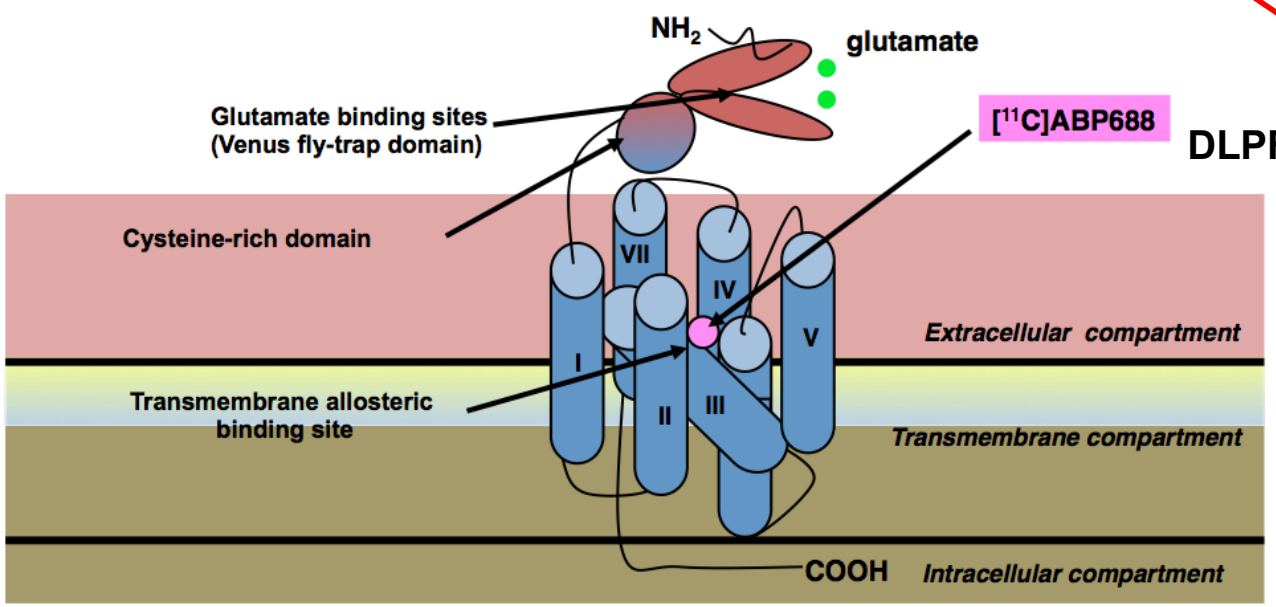

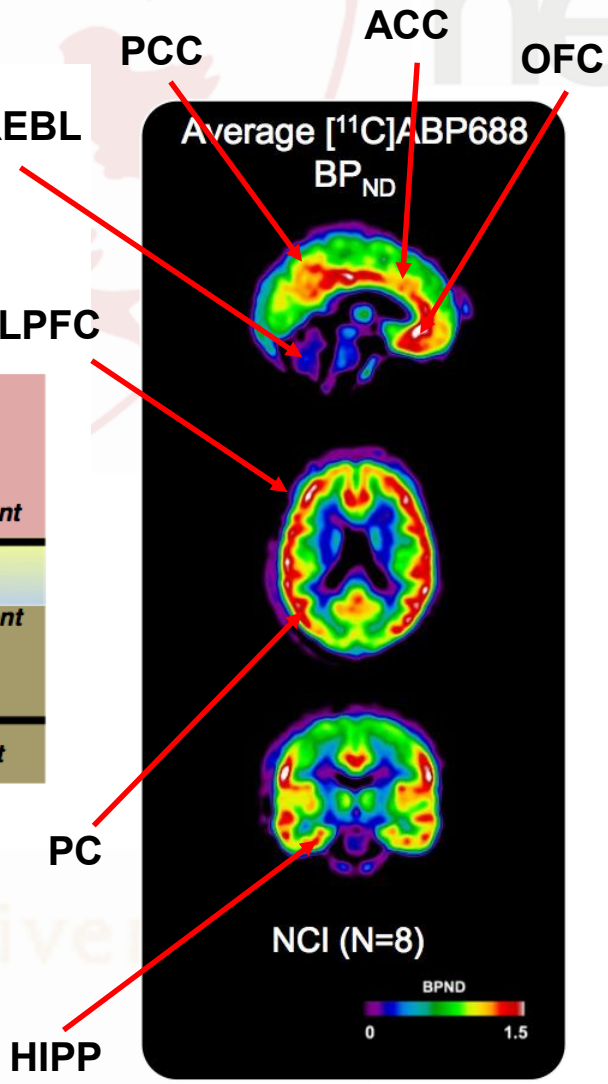

Orthostatic binding site: glutamate

Allosteric binding site: [^{11}C]ABP688

In vivo characterization of metabotropic glutamate receptor type 5 abnormalities in behavioral variant FTD

Brain Struct Funct
DOI 10.1007/s00429-014-0978-3

Antoine Leuzy · Eduardo Rigon Zimmer · Jonathan Dubois · Jens Pruessner · Cory Cooperman · Jean-Paul Soucy · Alexey Kostikov · Esther Schirmaccher · René Désautels · Serge Gauthier · Pedro Rosa-Neto

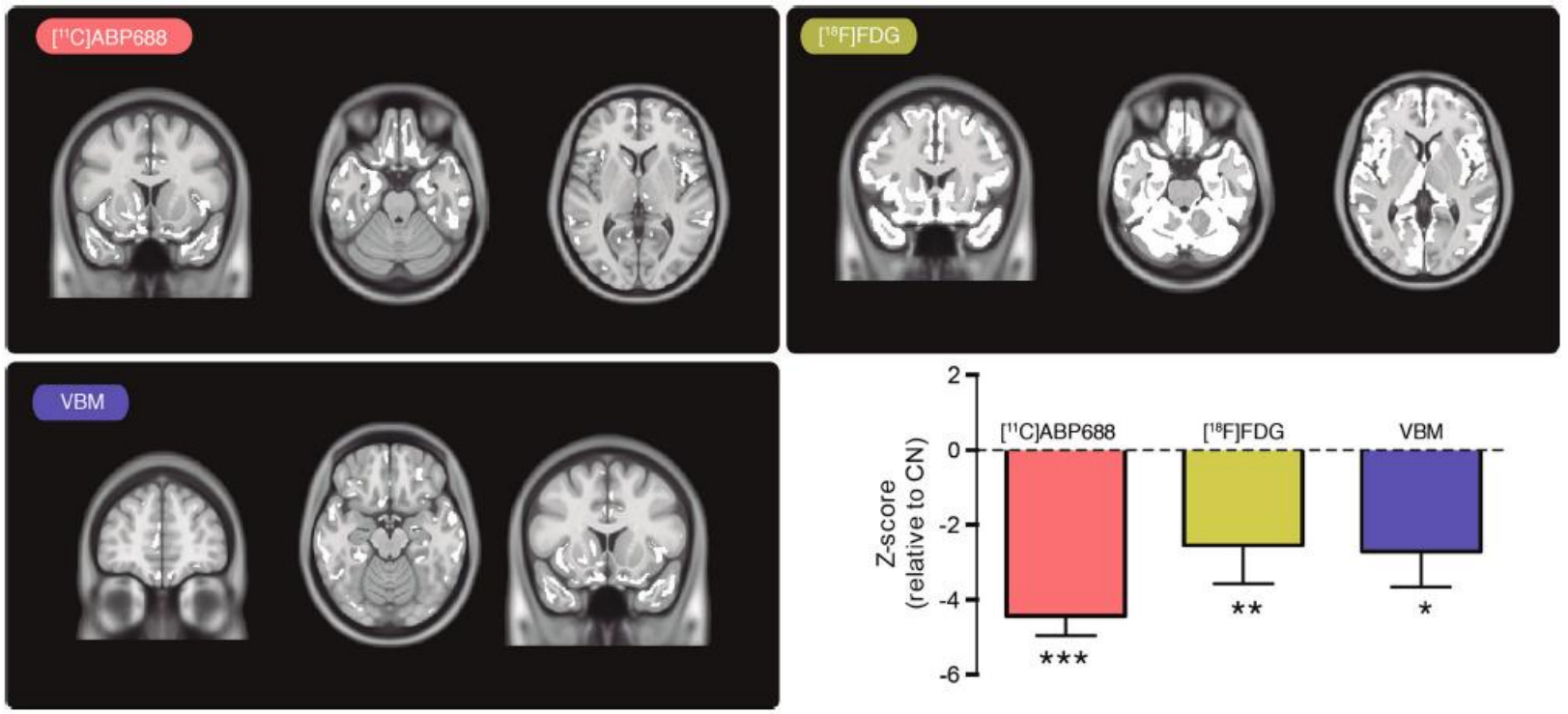

Fig. 1 *Z* score maps for all bvFTD patients were created for [^{11}C]ABP688 BP_{ND}, [^{18}F]FDG SUV_R, and VBM. These maps were then combined to show areas with significantly reduced [^{11}C]ABP688 BP_{ND}, [^{18}F]FDG SUV_R, and GM common to all bvFTD patients (*top left*, *top right*, *bottom left*, respectively). These common *Z* maps were then used to extract raw [^{11}C]ABP688 BP_{ND}, [^{18}F]FDG SUV_R, and VBM values. After conversion to *Z* scores, values were plotted, relative to CN subjects (*bottom right*). $***p < 0.001$, $**p < 0.01$, $*p < 0.05$

But the competition never sleeps!!

An amyloid ligand-free optical retinal imaging method to predict cerebral amyloid PET status

Jean-Paul Soucy[1,1a], Claudia Chevrefils[2], Jean-Philippe Sylvestre[2], Jean Daniel Arbour[3], Marc-André-Rhéaume[3], Sylvain Beaulieu[4], Céline Chayer[4], Alain Robillard[4], Pedro Rosa-Neto[1,5,6], Tharick A. Pascoal[1,5], Sulantha S. Mathotaarachchi[1,5], Ziad S. Nasreddine[7], Serge Gauthier[6], Frédéric Lesage[8]

[1,1a]McConnell Brain Imaging Centre, Montreal Neurological Institute, McGill University & PERFORM Centre, Montreal, Canada; [2]Optina Diagnostics, Montreal, QC, Canada; [3]Clinique ophtalmologique 2121, Montreal, Canada; [4] Hôpital Maisonneuve-Rosemont, Montreal, Canada; [5]Translational Neuroimaging Laboratory, McGill Centre for Studies in Aging, Douglas Mental Health University Institute, Montreal, Canada; [6]Alzheimer's Disease Research Unit, The McGill University Research Centre for Studies in Aging, McGill University, Montreal, Canada; [7]MoCA Clinic and Institute, Greenfield Park, Canada; [8]École Polytechnique de Montréal, Institut de génie biomédical, Département de Génie électrique, Montreal, Canada

Background

Screening method for early Aβ detection needed because:

- **Clear shift to test disease modifying drugs at preclinical phase of Alzheimer's disease (AD)**
- **Aβ used as a biomarker:** - **Essential** component of AD
  - **Sufficient** to classify on AD continuum
- **Current methods to identify Aβ *are not adapted for screening purposes***

Amyloid PET scan

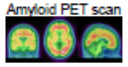

- Injection of radioactive tracer
- Costly
- Availability issues

CSF biomarkers

- Invasive lumbar puncture
- Availability issues
- Technical implementation issues

- **The problem-an example: recruitment of 3000 asymptomatic Aβ+ subjects:**

~12 000 PET scans required @5-10K$ = $ 60-120M to build cohort

A screening method could impact AD drug development by reducing cost and facilitating recruitment

Hyperspectral retinal imaging to identify biomarkers

Images of the retina in a series of wavelengths are obtained with the Metabolic Hyperspectral Retinal Camera (MHRC) delivering a dataset with spectral information at each pixel [1].

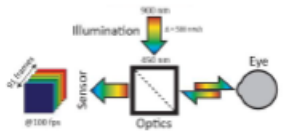

Retinal images at different wavelengths

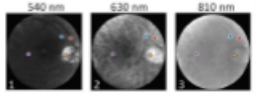

Varying spectral characteristics are obtained for different points chosen in tissue and may be used to discriminate properties of the retina [2].

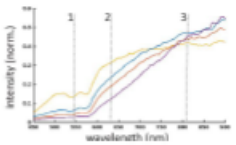

Evidence of Aβ was previously observed with hyperspectral imaging in the retina of mice *ex vivo* and *in vivo*. [3, 4]

Main objective

In this pilot study, a non-invasive retina imaging approach with the MHRC is evaluated as a proxy to identify biomarkers which correlate with the cerebral load of amyloid plaques.

MHRC retina images

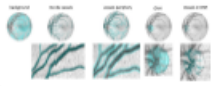

Equivalence?

Cerebral amyloid PET

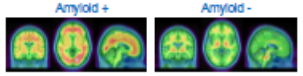

Methods

Study cohort

- 45 volunteers (16 probable AD and 29 age-matched controls)
- Age range 53 to 85 years
- Probable AD status as determined by clinical evaluation
  - MMSE between 20 and 26, inclusively
  - Hachinski Ischemia Score below 4
  - Sufficient degree of cooperation to participate
- Controls with no clinical sign of cognitive impairment (MoCA of 26 or higher)
- No concomitant retinal disease (retinopathy, glaucoma or macular degeneration)
- No significant media opacity (natural or intra-ocular lens)
- Achievable good pupil dilation (≥ 6mm) and good visual fixation

Study design

Cognitive evaluation → Pupil dilation & Ophthalmological examination → MHRC acquisition in reflectance (450-900 nm in steps of 5 nm) → Amyloid PET imaging with ^{18}F-Florbetaben to determine amyloid status (visual assessment)

Hyperspectral image processing

- Reflectance datasets are registered and normalized to extract meaningful spectral information
- Spatial/spectral texture maps are built to evaluate features in the datasets invisible to the naked eye

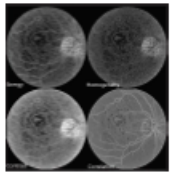

- Image segmentation of specific regions of interest (ROI) in the retina (in particular the principal retinal vessels)
- Calculation of first order statistics for the ROI (16 features)

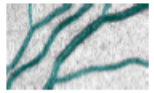

Amyloid status prediction using machine learning

- 112 hyperspectral datasets from the 45 subjects (1-3 per subjects)
- Supervised classification of the retinal texture features based on the PET amyloid status is performed
- Classification performance is estimated using Leave One Out Cross Validation

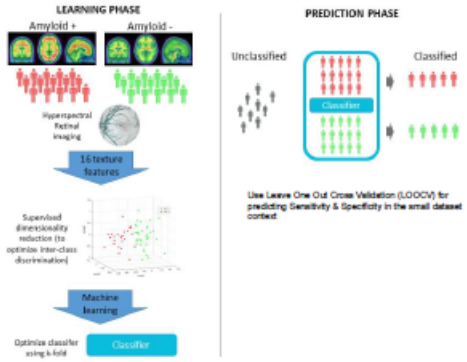

Results

Amyloid PET status

Amyloid PET status determined by visual assessment from a panel of 3 readers with a panel review to discuss cases with discrepancy between readers after initial reading. Consensus was reached for 44 cases and the majority read was used for the only case without consensus.

Consistent with literature reports:

- 2 of 16 probable AD subjects are Aβ-
- 5 of 29 cognitively normal subjects are Aβ+

Retinal Imaging & Classification

- At least one good retinal acquired with the MHRC in the vast majority of the participants enrolled in the study (45/47)
- Excellent retinal scanning correspondence with PET amyloid status achieved when the ROI is inside the large retinal vessels

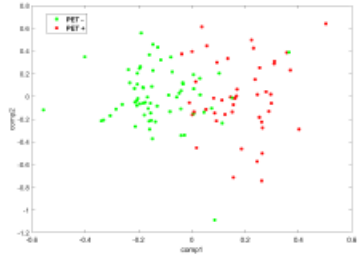

sensitivity:84%
specificity: 86%
(estimated using LOOCV)

- **A cohort of 3000 asymptomatic Aβ+ subjects (confirmed by amyloid PET) could be built with < 3500 PET scans using the retinal scan as a screening tool**

Conclusions

- **The developed machine learning approach, based on hyperspectral retinal imaging, shows promise in predicting cerebral amyloid PET status and could serve as a screening tool to identify subjects in the early stages of the AD continuum, for instance in a drug development context.**
- **Multi-site study underway to test the approach in more subjects**

Acknowledgements/ Disclosures

- Volunteers who participated in this study
- Staff at the Clinique Ophtalmologique 2121, MoCA Clinic and Institute and VM Medical Clinic
- Members of the Optina team
- The CQDM Focus on Brain program for funding
- Commercial relationships: C.C., J.-P.Sy. and J.D.A. with Optina Diagnostics

1. Patel et al., IOVS (2013) 54: 5163-5168
2. Desjardins et al., Exp Eye Res (2016) 145: 330-340.
3. More et al., ACS Chem Neurosci (2015) 6: 306-315.
4. More et al., IOVS (2016) 7: 3231-3238

Accurate risk estimation of β-amyloid positivity to identify prodromal Alzheimer's disease: Cross-validation study of practical algorithms

Alzheimer's & Dementia https://doi.org/10.1016/j.jalz.2018.08.014

Sebastian Palmqvist[a,b,*], Philip S. Insel[a], Henrik Zetterberg[c,d,e,f], Kaj Blennow[c,d], Britta Brix[g], Erik Stomrud[a,h], the Alzheimer's Disease Neuroimaging Initiative[1], the Swedish BioFINDER study, Niklas Mattsson[a,b], Oskar Hansson[a,h,**]

Introduction: The aim was to create readily available algorithms that estimate the individual risk of β-amyloid (Aβ) positivity.

Methods: The algorithms were tested in BioFINDER (n = 391, subjective cognitive decline or mild cognitive impairment) and validated in Alzheimer's Disease Neuroimaging Initiative (n = 661, subjective cognitive decline or mild cognitive impairment). The examined predictors of Aβ status were demographics; cognitive tests; white matter lesions; apolipoprotein E (*APOE*); and plasma $A\beta_{42}/A\beta_{40}$, tau, and neurofilament light.

Results: Aβ status was accurately estimated in BioFINDER using age, 10-word delayed recall or Mini–Mental State Examination, and *APOE* (area under the receiver operating characteristics curve = 0.81 [0.77–0.85] to 0.83 [0.79–0.87]). When validated, the models performed almost identical in Alzheimer's Disease Neuroimaging Initiative (area under the receiver operating characteristics curve = 0.80–0.82) and within different age, subjective cognitive decline, and mild cognitive impairment populations. Plasma $A\beta_{42}/A\beta_{40}$ improved the models slightly.

Discussion: The algorithms are implemented on http://amyloidrisk.com where the individual probability of being Aβ positive can be calculated. This is useful in the workup of prodromal Alzheimer's disease and can reduce the number needed to screen in Alzheimer's disease trials.

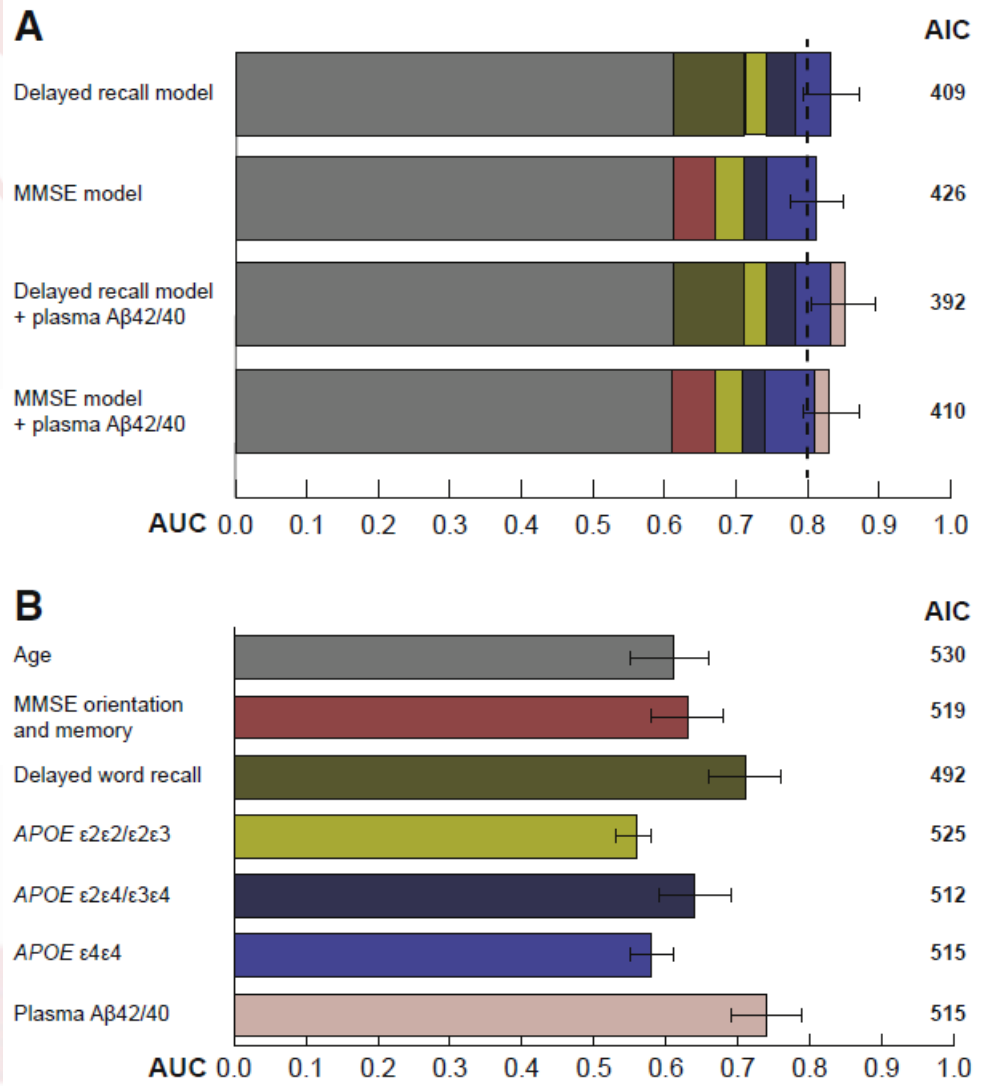

Bermejo-Pareja *et al. BMC Neurology* 2010, **10**:108
http://www.biomedcentral.com/1471-2377/10/108

BMC Neurology

RESEARCH ARTICLE Open Access

Saliva levels of Abeta1-42 as potential biomarker of Alzheimer's disease: a pilot study

Felix Bermejo-Pareja[1,2], Desiree Antequera[2,3], Teo Vargas[2,3], Jose A Molina[1,2], Eva Carro[2,3*]

Journal of Alzheimer's Disease 27 (2014) 299–305
DOI 10.3233/JAD-2011-110731
IOS Press

Salivary Tau Species are Potential Biomarkers of Alzheimer's Disease

Min Shi[a], Yu-Ting Sui[a], Elaine R. Peskind[b,c], Ge Li[b], HyeJin Hwang[a], Ivana Devic[a], Carmen Ginghina[a], John Scott Edgar[d], Catherine Pan[a], David R. Goodlett[d], Amy R. Furay[a,b], Luis F. Gonzalez-Cuyar[a] and Jing Zhang[a,*]

We can also use some help on the equipment side …

GATE Simulation of a Fully Pixelated Ultra-High Resolution Brain PET Scanner

November 14TH, 2018 – M05-05

Émilie Gaudin[1], Maxime Toussaint[2], Christian Thibaudeau[3], Maxime Paille[1], Réjean Fontaine[4] and Roger Lecomte[1,3]

[1]Sherbrooke Molecular Imaging Center of CRCHUS & Dept. of Nuclear Medicine and Radiobiology, Université de Sherbrooke, QC, Canada
[2]Department of Computer Science, Université de Sherbrooke, QC, Canada
[3]IR&T Inc., Sherbrooke, QC, Canada
[4]Institut Interdisciplinaire d'Innovation Technologique (3IT) & Department of Electrical and Computer Engineering, Université de Sherbrooke, QC, Canada

UNIVERSITÉ DE SHERBROOKE

CIMS Centre d'imagerie moléculaire de Sherbrooke

GRAMS

IR&T Imaging Research and Technology

Sydney IEEE NSS/MIC 2018

Performance comparison

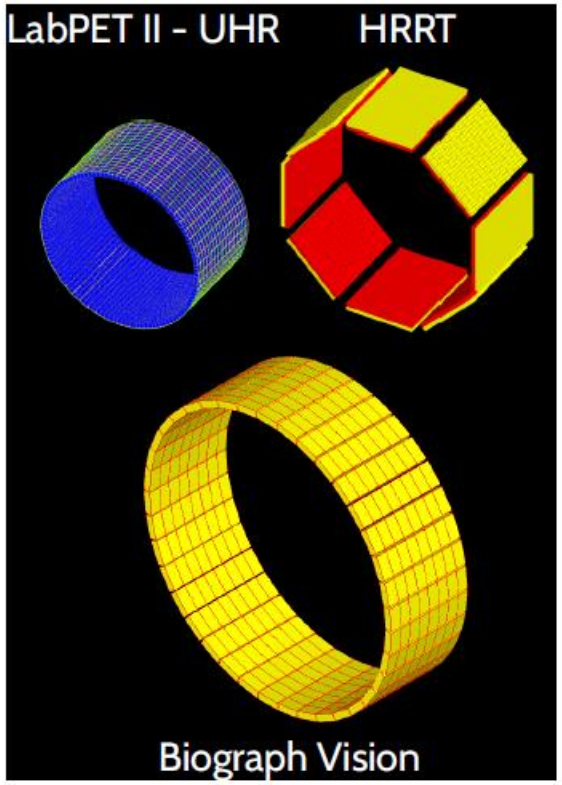

System Parameters	UHR	HRRT [8]	Vision [9]
Photodetector	APD	PMT	SiPM
Scintillator material	LYSO	LSO/LYSO	LSO
# scintillators	129,024	119,880	60,800
Scintillator size (mm^3)	1.12×1.12×12	2.1×2.1× 20	3.2×3.2×20
Sharing ratio	1:1	7488:140	200:128
Ring diameter (mm)	390	469	820
Axial length (mm)	235	252	263
Transaxial FOV (mm)	271	312	700
Time window (ns)	6	6	4.73
Energy window (keV)	250–650	350–650	435–650

[8] H. W. A. M. de Jong et al. (2007). *Physics in Medicine & Biology* 52 (5), p. 1505

[9] (2016). Siemens Healthcare GmbH

Imaging Performance

Hot spot phantom

- Uniform ^{18}F activity concentration: 200 kBq/cc
- Reconstruction 30 iter.

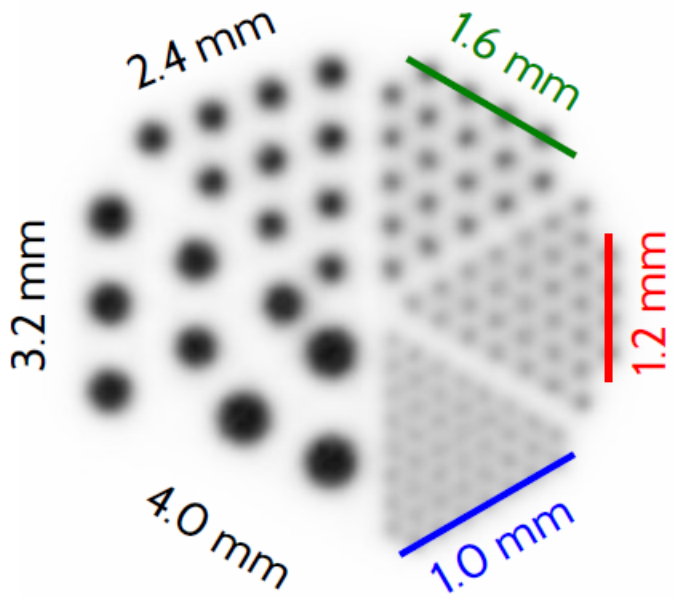

Contrast:

$$C = \frac{I_0 - I_B}{I_B}$$

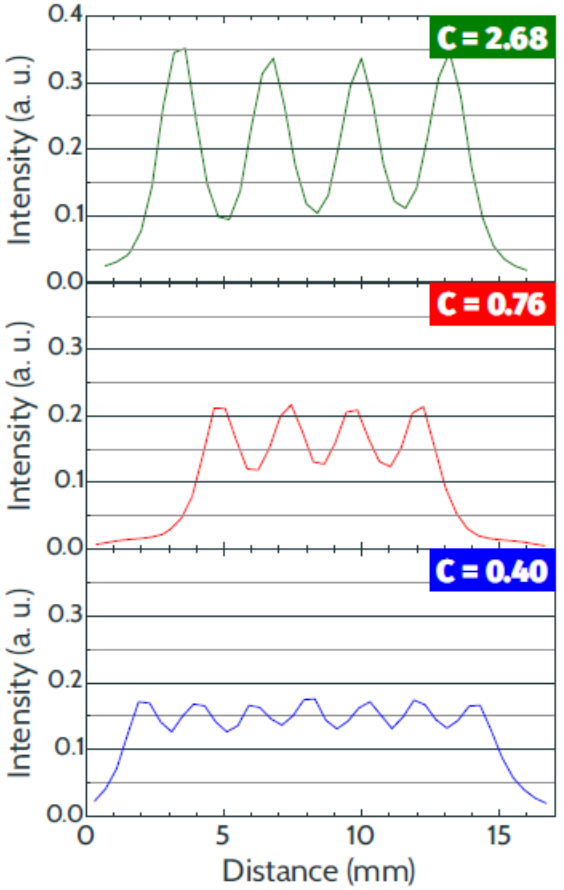

Brain phantom imaging

MRI-based Zubal phantom [10] - **1.5 mm voxel dimension** - 256 × 256 × 128 matrix
^{18}F source - 30 iter. - Gaussian filter FWHM 1 mm

UHR	HRRT	Biograph Vision
		
420 × 10^6 events	477 × 10^6 events	538 × 10^6 events
1.12×1.12×12 mm^3 pixel	2.1×2.1×20 mm^3 pixel	3.2×3.2×20 mm^3 pixel
Resolution 1.32 mm	Resolution 2.4 mm	Resolution 3.4 mm

[10] I. G. Zubal et al. (1994). *Medical Physics* 21 (2), pp. 299–302

Et caetera!

(MRI, Plasma markers, CSF markers, …)

So, how will we do??

I don’t really know because the data just isn’t available!

But I do believe that molecular imaging will do well by providing specific identification of diseases which will be needed for personalized medicine purposes.

2018 National Institute on Aging—Alzheimer's Association (NIA-AA) Research Framework

NIA-AA Framework: Toward a biological definition of Alzheimer's disease

Alzheimer's & Dementia 14 (2018) 535-562

Clifford R. Jack, Jr.,[a,*], David A. Bennett[b], Kaj Blennow[c], Maria C. Carrillo[d], Billy Dunn[e], Samantha Budd Haeberlein[f], David M. Holtzman[g], William Jagust[h], Frank Jessen[i], Jason Karlawish[j], Enchi Liu[k], Jose Luis Molinuevo[l], Thomas Montine[m], Creighton Phelps[n], Katherine P. Rankin[o], Christopher C. Rowe[p], Philip Scheltens[q], Eric Siemers[r], Heather M. Snyder[d], Reisa Sperling[s]

Contributors[†]: Cerise Elliott, Eliezer Masliah, Laurie Ryan, and Nina Silverberg

Biomarker profiles and categories

AT(N) profiles	Biomarker category	
A-T-(N)-	Normal AD biomarkers	
A+T-(N)-	Alzheimer's pathologic change	Alzheimer's continuum
A+T+(N)-	Alzheimer's disease	
A+T+(N)+	Alzheimer's disease	
A+T-(N)+	Alzheimer's and concomitant suspected non Alzheimer's pathologic change	
A-T+(N)-	Non-AD pathologic change	
A-T-(N)+	Non-AD pathologic change	
A-T+(N)+	Non-AD pathologic change	

AMYLOID
TAU
NEURODEGENERATION
(including ^{18}FDG)

No place for symptoms!!!

Molecular Imaging rules!!!

CHUM

neuro

Concordia University
PERFORM

CHUM

neuro

Concordia University
PERFORM

Le ^{18}F-FDG se comporte «comme» le glucose; il en découle que …

Étude TEP-^{18}F-FDG:
Données brutes

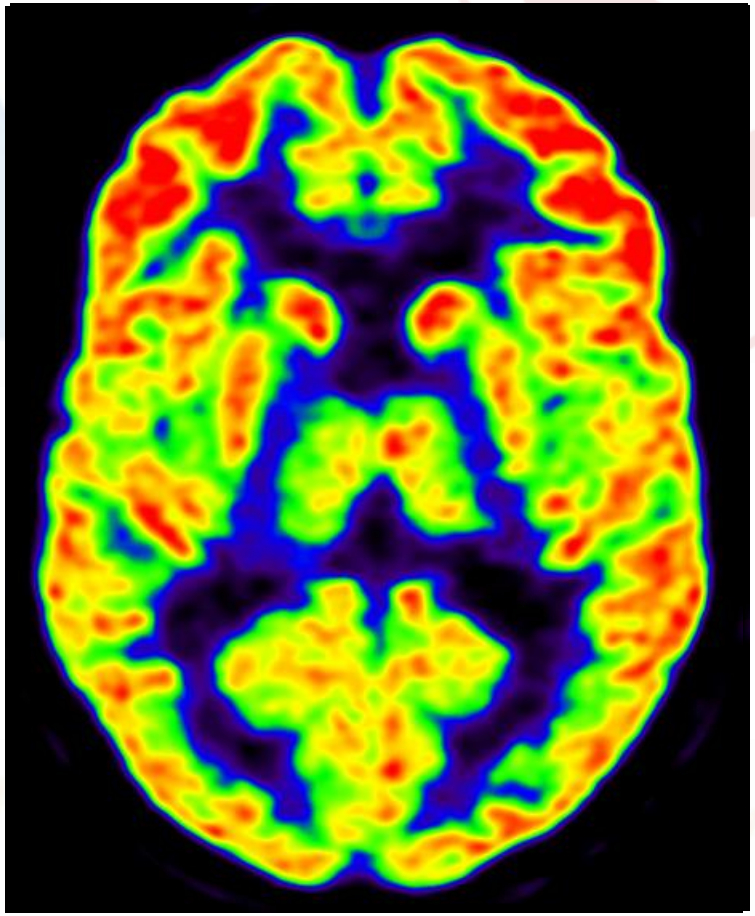

Distribution RELATIVE de la radioactivité

Échange glutamate-glucose

Comment est glutamatergique ?

Antib … in mc … d beta … e

Dag Sehlin[1] … vänen[1]

… 3/ncomms10759
2017

Owing to the … positron emi… targets in pe… limited by th… diagnosis an… antibody mA… receptor-mec… with Aβ path… correlates cl… ligands can b…

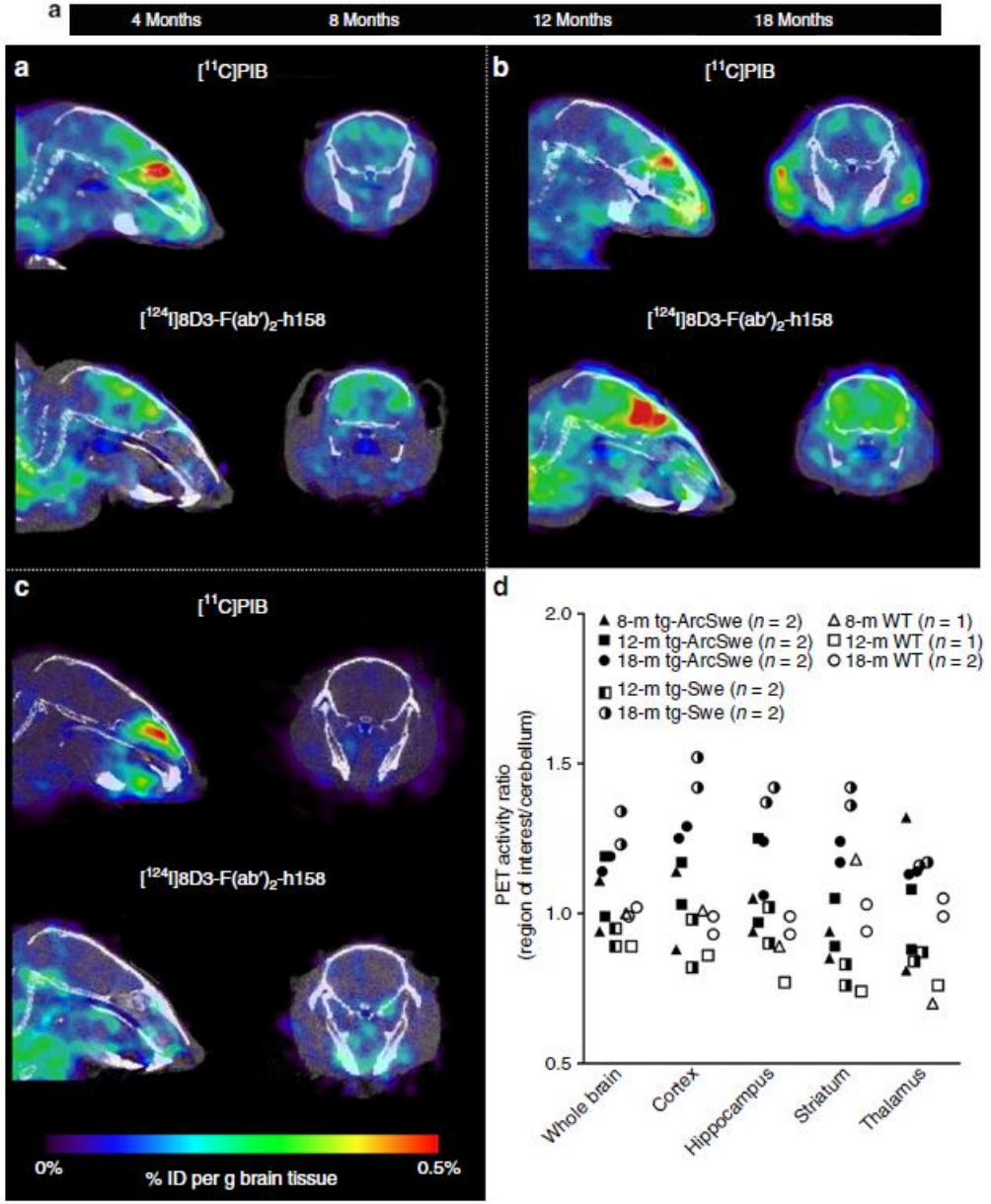

Figure 7 | Comparison of PET imaging with [^{11}C]PIB- and ^{124}I-labelled fusion protein in transgenic and WT mice. PET images obtained during 60 min 72 h after injection of [^{124}I]8D3-F(ab')$_2$-h158, or during 20 min, starting 40 min after injection of [^{11}C]PIB. Transverse and sagittal views of one representative 18-month-old tg-ArcSwe (**a**), tg-Swe (**b**) and WT (**c**) mouse with the two radioligands. (**d**) PET image-based quantification of brain distribution of [^{11}C]PIB relative to that in cerebellum for tg-ArcSwe, tg-Swe and WT mice in the different age groups (each symbol represents one animal). Representative PET images are shown in **a**–**c**. Number of animals included in each group is shown in **d**.

above, demonstrating low and equal brain uptake in 18-month-old WT and tg-ArcSwe mice. Representative PET images are shown in **a**,**c** and **d**. Number of animals included in each group is shown in **b**.